
RESULTS
&
DISCUSSION

SECTION (A)

STUDYING THE CORROSION BEHAVIOR OF ALUMINUM BY THE CHEMICAL TECHNIQUE

To evaluate the influence of the investigated compounds on the corrosion of aluminum in 1M hydrochloric acid, the weight loss technique was employed as the chemical testing technique for aluminum pure only .

3.1-Corrosion inhibition behavior

The corrosion behavior of a metal in aqueous environment is characterized by the extent to which it dissolves in the solution. This can be quantified by using the simple relationship described before (2.1).

The degree of dissolution, of course, dependent on the surface area of the metal exposed and the time of exposure; hence the amount of corrosion is given with respect to area and time. The resulting quantity, corrosion rate, is thus a fundamental measurement in corrosion science. Corrosion rates can be evaluated by measuring either the concentration of the dissolved metal in solution by chemical analysis or by measuring weight of a specimen before and after exposure and applying equation (2.1). The later is most common method. The weight loss method is usually preferred because the quantity measured is directly related to the extent of corrosion and does not rely on any assumptions about reactions occurring during corrosion.

Figs. (3.1-3.2) show the weight loss- time curves for the corrosion of aluminum in 1 M hydrochloric acid in the absence and presence of different concentrations of the investigated compounds at 30±1^{o}C . , the weight loss of aluminum samples are decreased. This means that the presence of these compounds retards the corrosion of aluminum in 1M hydrochloric acid or in other words, these compounds act as inhibitors.

The linear variation of weight loss with time in uninhibited and inhibited 1M hydrochloric acid indicates the absence of insoluble surface films during corrosion. In the absence of any surface films, the inhibitors are first adsorbed onto the metal surface and thereafter impede corrosion either by merely blocking the reaction sites (anodic and cathodic) or by altering the mechanism of the anodic and cathodic partial processes.

The percentage inhibition efficiency (%IE) of the investigated compounds was determined using the equation mentioned before (2.2).

From the calculated values of % IE at $30^{o}C$ as shown in Table (3.1), the order of decreasing inhibition efficiency of the investigated compounds is as follows:

Compound (I) > compound (II)

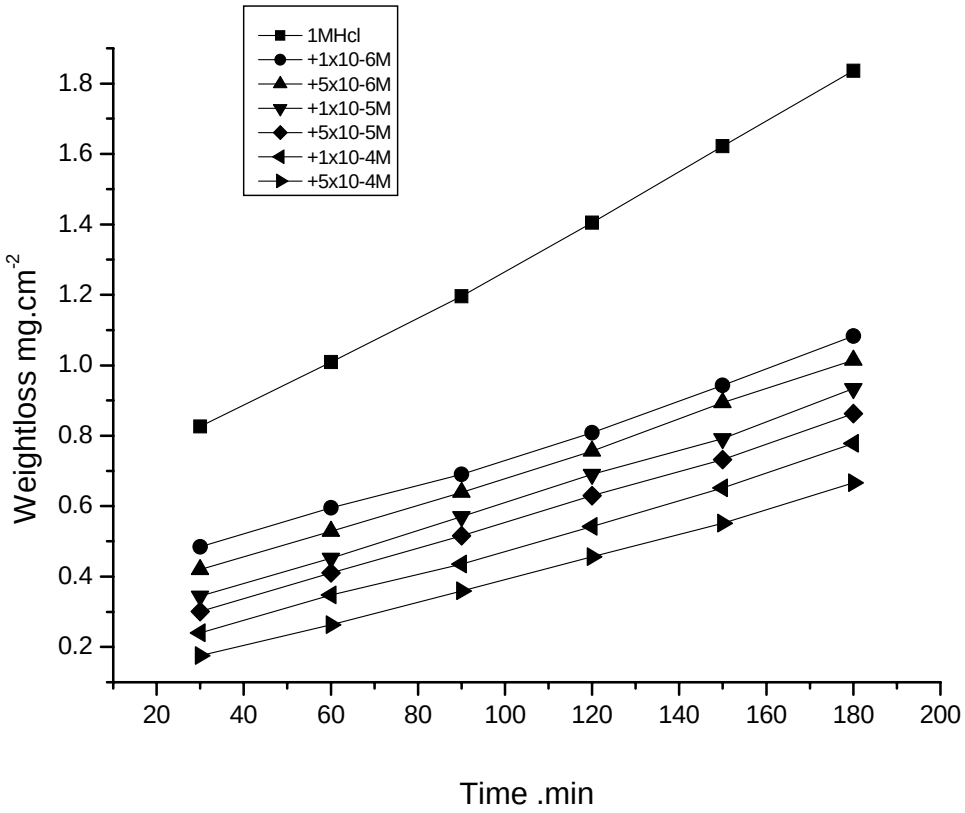

Fig(3.1):Weight loss -time curves for the corrosion of aluminum in 1 M HCl in the absence and presence of different concentrations of compound(I) at 30 ^{o}C.

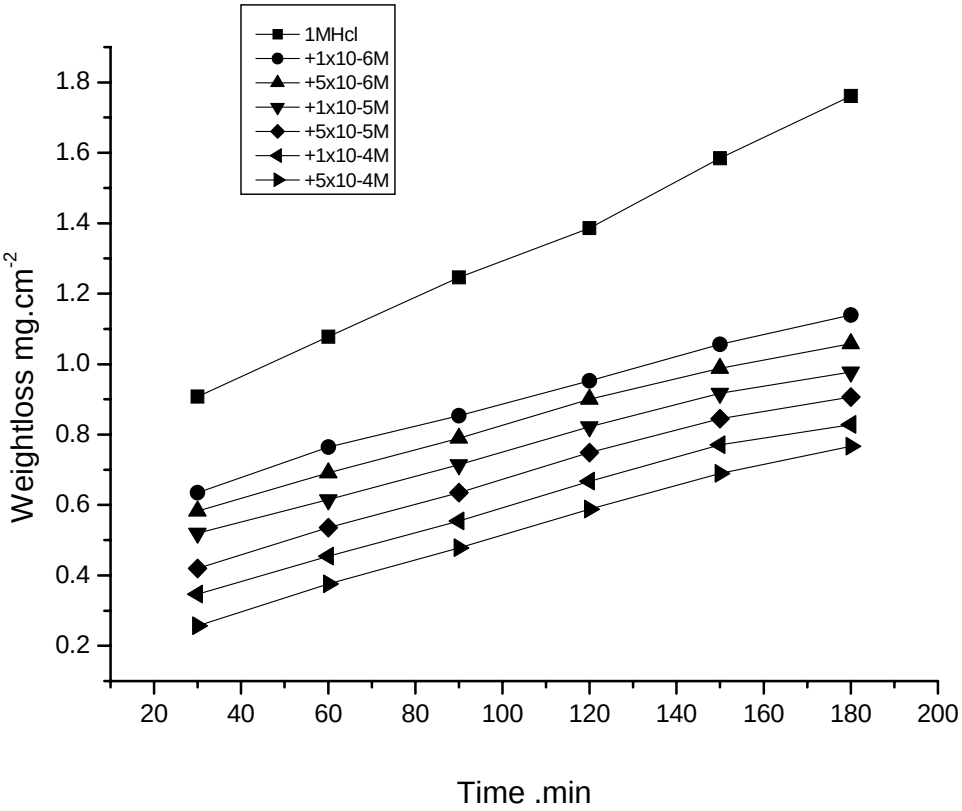

Fig(3.1):Weight loss -time curves for the corrosion of aluminum in 1 M HCl in the absence and presence of different concentrations of compound (II) at 30 ^{o}C.

Table (3.1): Inhibition efficiency (%IE) of aluminum dissolution in1M HCl in the presence of different concentrations of investigated compounds at 30 ^{0}C and 120 min immersion.

Concentration M	**% Inhibition efficiency (IE%)**	
	Compound (I)	Compound (II)
$1x10^{-6}$	٤٣,٧٨	٤٠,٥٤
$5x10^{-6}$	٥١,٣٥	٤٧,٠٣
$1x10^{-5}$	٥٢,٤٣	٥٠,٨١
$5x10^{-5}$	٥٧,٣٩	٥١,٤٥
$1x10^{-4}$	٦٢,١٦	٦٢,٠١
$5x10^{-4}$	٦٨,١١	٦٧,٥٧

3.2. Role of Anions in Corrosion Inhibition of Aluminum in Acid Solution and their Synergistic Effect.

The effect of I^-, SCN^- and Br^- ions on the corrosion- inhibition of aluminum in 1M HCl solution in the presence and absence of investigated compounds was studied by the weight loss method .

Figs. (3.3-3.8) represent the weight loss-time curves for aluminum dissolution in 1 M HCl in the presence of 10^{-2} M I^-, SCN^-, Br^-,and also in presence of different concentrations of compounds .

The values of inhibition efficiency (%IE) for various concentrations of inhibitors in the presence of specific concentration of these anions are given in Tables (3.2-3.4).

It is observed that (%IE) of the inhibitors increases on addition of these different anions due to synergistic effects [137] . The strong chemisorptions of these anions on the metal surface is responsible for the synergistic effect of these ions. Competitive adsorption of anions (I^-, **SCN^-,** Br^-) and inhibitors anions was considered.

The synergistic inhibition effect was evaluated using a parameter S_θ obtained from the surface coverage values (θ) of the anions,cations and both. Aramaki and Heckerman [138] calculated the synergism parameter S_θ using the following equation:

$$S_\theta = 1-\theta_{1+2}/1-\theta^-_{1+2} \qquad (3.1)$$

Where

$\theta_{1+2}=(\theta_1+\theta_2)-(\theta_1\theta_2)$

θ_1=surface coverage by anion .

θ_2=surface coverage by cation.

θ^-_{1+2}= measured surface coverage by both the anion and cation.`

We calculate synergism parameters from the above equation. The plot of the synergism parameter (S_θ) against various concentrations of compounds given in Figs. (3.9-3.15) and the corresponding values are shown in . Tables (3.5-3.7). As can be seen from these Tables, values nearly equal to unity, which suggests that the enhanced inhibition efficiencies caused by the addition of these anions to investigated compounds is due mainly to the synergistic effect.

Synergistic adsorption is classified into three types plus a mixture of the above two:

(i) Specific co -adsorption of anions and cations.

(ii) Ionic or physical overlap adsorption of cations over the anion covered

aluminum surface.

(iii) Mixture of the above two.

From previous results it is known that KI would be considered as one of the effective anions for synergistic action within the investigated salts.

The net increment of inhibition efficiency shows a synergistic effect of KI , KSCN, KBr, with investigated compounds, the synergistic effect depends on the type and concentration of anions .

The adsorption ability on the aluminum surfaces was in the order

KI > KSCN >*KB r* [(139).]

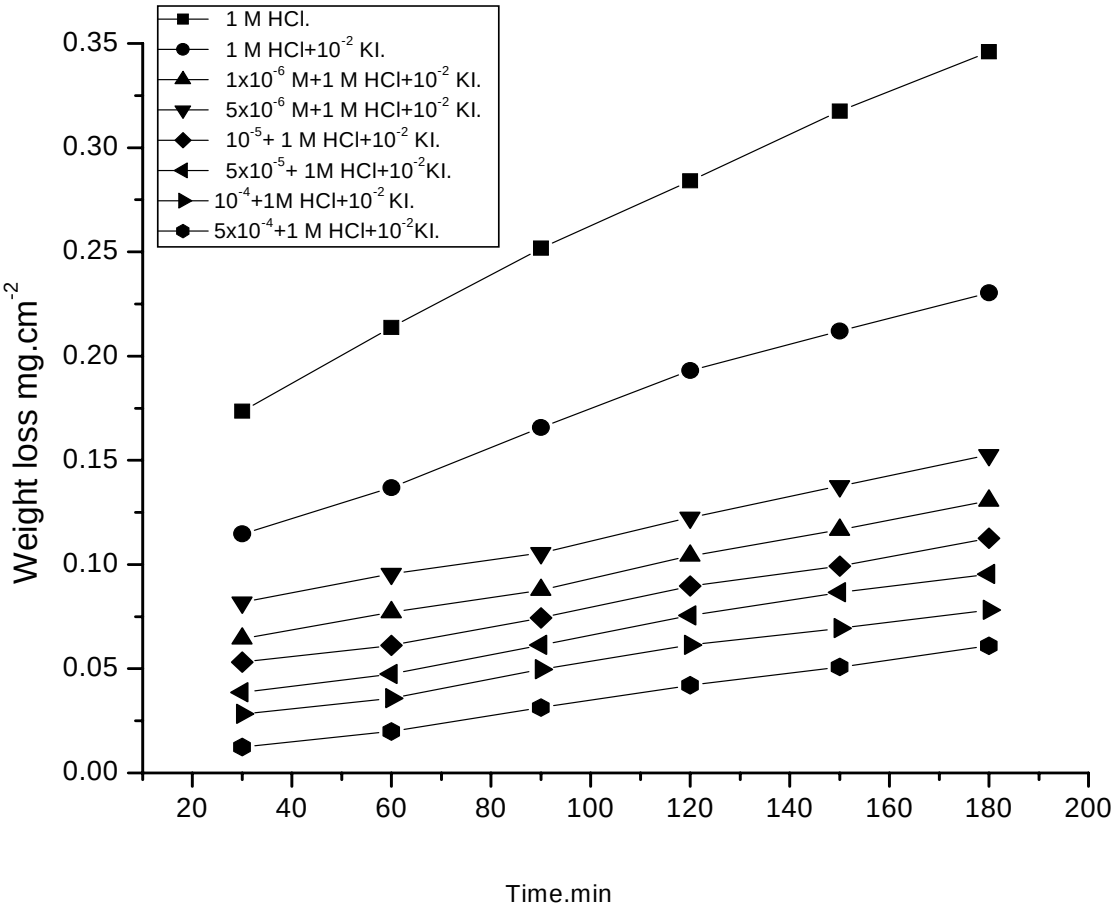

Fig (3.3): Weight loss-time curves for aluminum dissolution in the absence and presence of diffrent concentrations of compound (I) without and with addition of $1x10^{-2}$M KI at 30 ^{o}C

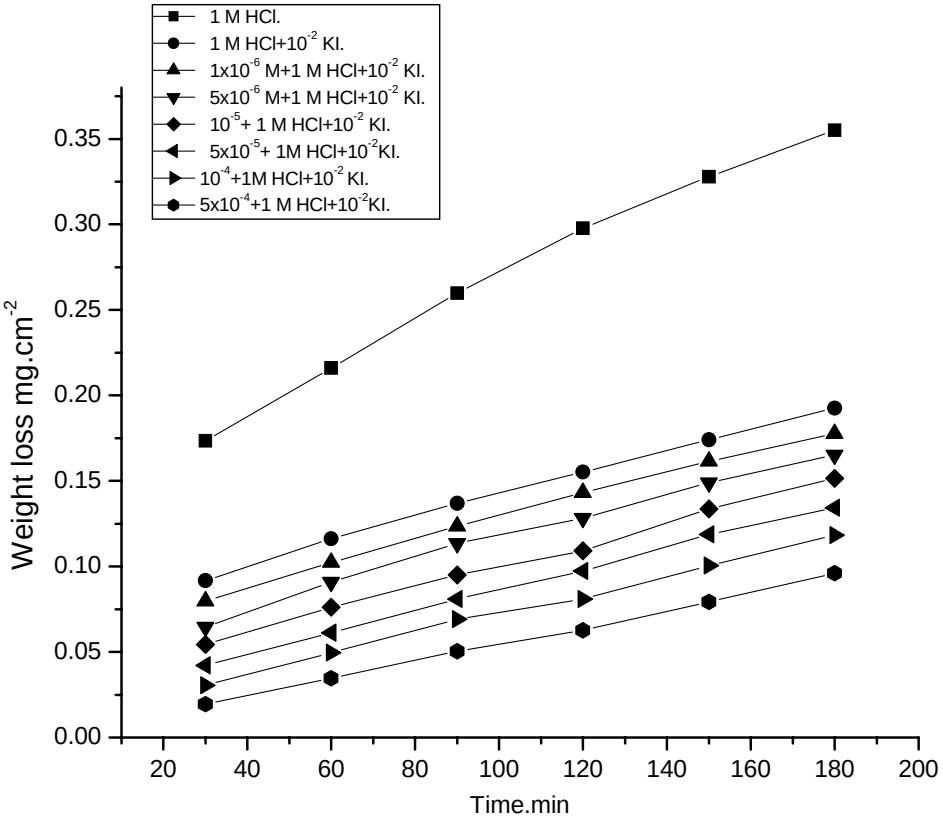

Fig (3.4): Weight loss-time curves for aluminum dissolution in 1 M HCl in the absence and presence of diffrent concentrations of compound(II) without and with addition of $1x10^{-2}$M KI at 30 ^{o} C

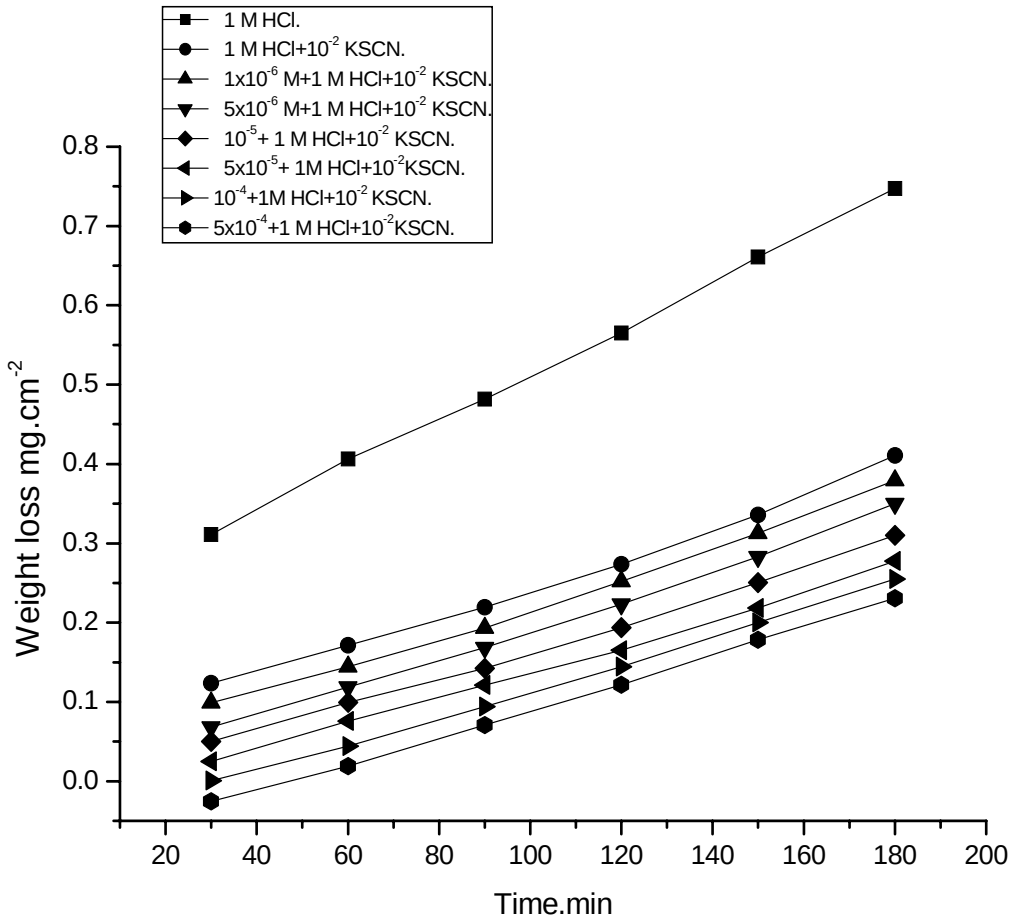

Fig.(3.5): Weight loss -time curves for aluminum dissolution in 1 M HCl in the absence and presence of different concentration of compound (I) without and with addition of $1x10^{-2}$M KSCN at 30 ^{o}C.

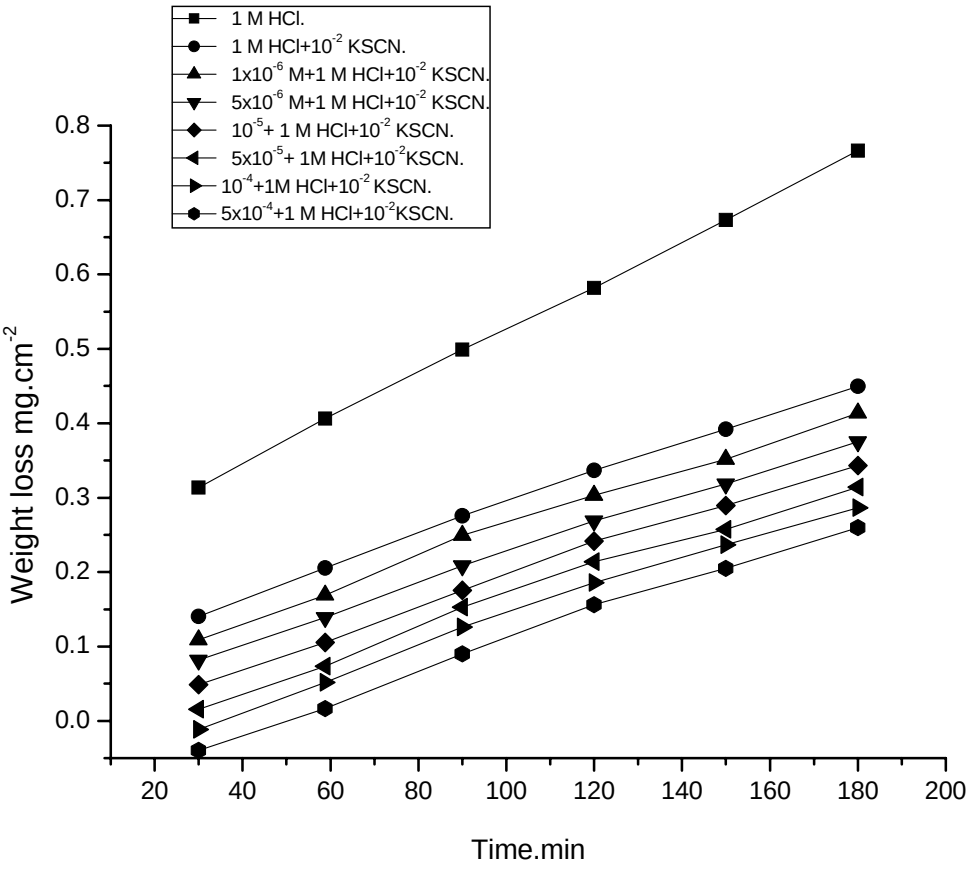

Fig.(3.6): Weight loss -time curves for aluminum dissolution in 1M HCl in the absence and presence of different concentration of compound (II) without and with addition of $1x10^{-2}$ KSCN at 30 ^{o} C.

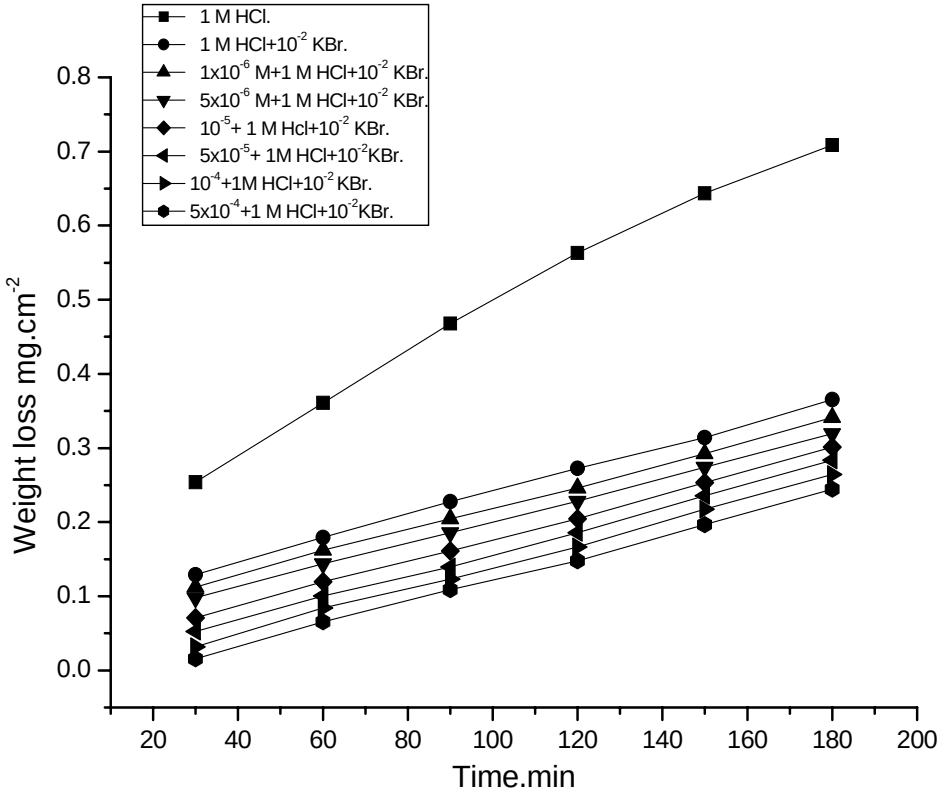

Fig.(3.7): Weight loss -time curves for aluminum dissolution in 1 M HCl in the absence and presence of different concentration of compound (I) without and with addition of $1x10^{-2}$M KBr at 30 ^{o}C.

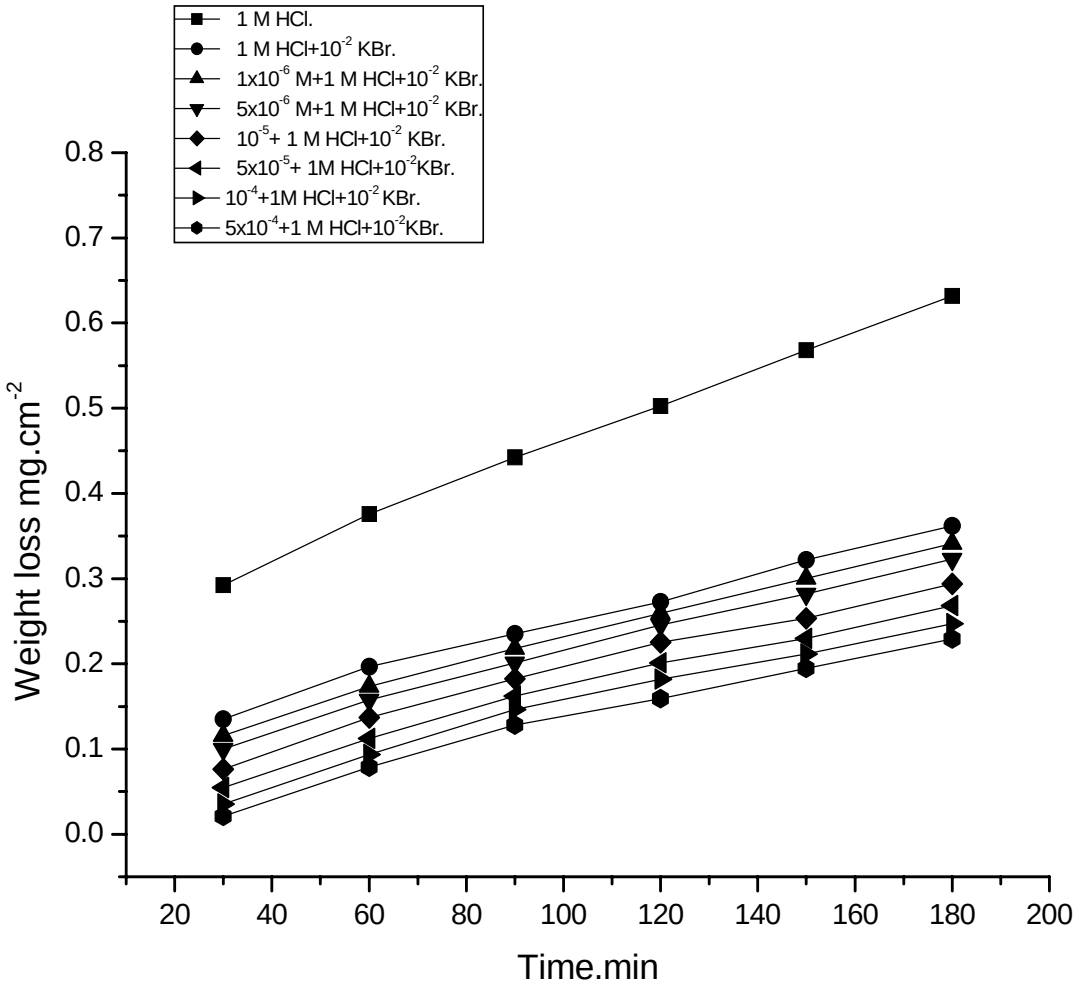

Fig.(3.8): Weight loss -time curves for aluminum dissolution in 1 M HCl in the absence and presence of different concentration of compound (II) without and with addition of $1x10^{-2}$M KBr at 30 ^{o}C.

Table(3.3): %Inhibition efficiency of aluminum dissolution in 1M HCl in presence of different concentration of the investigated compounds with addition of $1x10^{-2}$ M KI at 30 ^{o}C and at 120 min immersion .

Concentration	**% Inhibition efficiency (% IE)**	
M	Compound(I)	Compound(II)
$1x10^{-6}$	٥٦,٢٥	٥٠,٠٠
$5x10^{-6}$	٦٥,٦٣	٥٠,٢١
$1x10^{-5}$	68.75	٥٣,١٣
$5x10^{-5}$	٧١,٨٨	٦٢,٥
$1x10^{-4}$	٧٣,١٣	٦٨,٧٥
$5x10^{-4}$	٧٥,٠٠	٧٤,٢٣

Table(3.3): %Inhibition efficiency of aluminum dissolution in 1M HCl in presence of different concentration of the investigated compounds with addition of $1x10^{-2}$ M KSCN at 30°C and at 120 min immersion .

Concentration	**% Inhibition efficiency (% IE)**	
M	Compound(I)	Compound(II)
$1x10^{-6}$	٥٠,٠٠	٤٤,٣٨
$5x10^{-6}$	٥٢,٨٦	٥٠,٠٠
$1x10^{-5}$	58.57	٥٢,٦٦
$5x10^{-5}$	٦١,٤٣	٥٧,١٤
$1x10^{-4}$	٦٥,٧١	٦٢,٢٩
$5x10^{-4}$	٧١,٤٣	٦٨,٥٧

Table (3.4): %Inhibition efficiency of aluminum dissolution in 1M HCl in presence of different concentration of the investigated compounds with addition of $1x10^{-2}$ M KBr at 30 ^{o}C and 120 min immersion.

Concentration M	**% Inhibition efficiency (% IE)**	
	Compound(I)	Compound(II)
$1x10^{-6}$	٥٢,٣١	٤٧,٦٩
$5x10^{-6}$	٥٥,٣٨	٥٠,٧٧
$1x10^{-5}$	٦٠,٠٠	٥٣,٨٥
$5x10^{-5}$	٦٣,٠٨	٥٨,٤٦
$1x10^{-4}$	٦٨,١٢	٦١,٥٤
$5x10^{-4}$	69.23	٦٧,٦٩

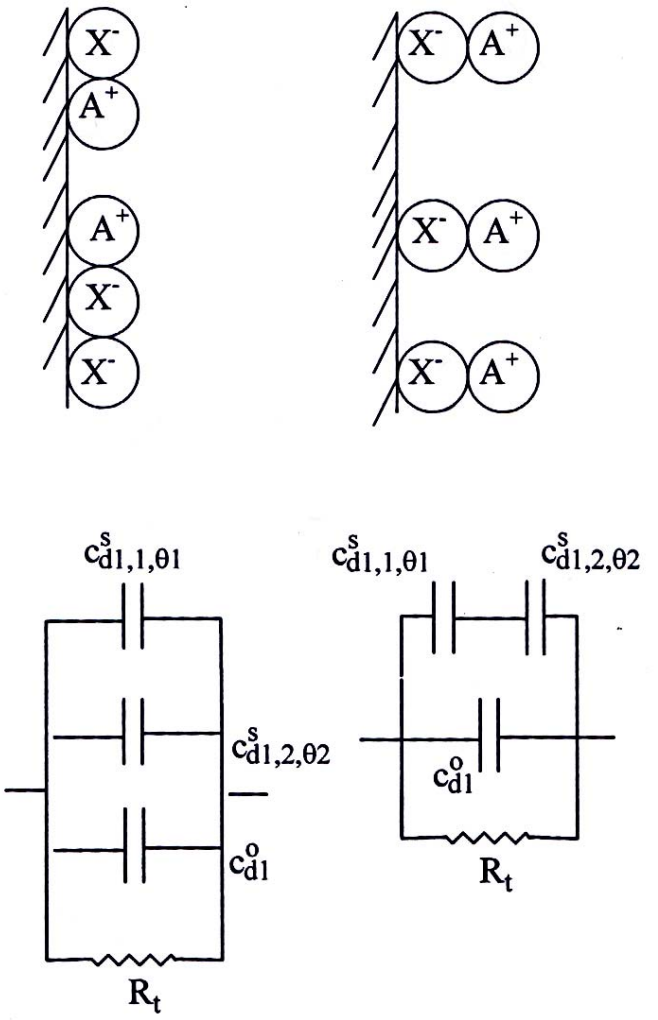

Competitive adsorption **Cooperative adsorption**

Fig. (3.9): Schematic diagrams and equivalent circuits of competitive and cooperative adsorption of anions and cation .

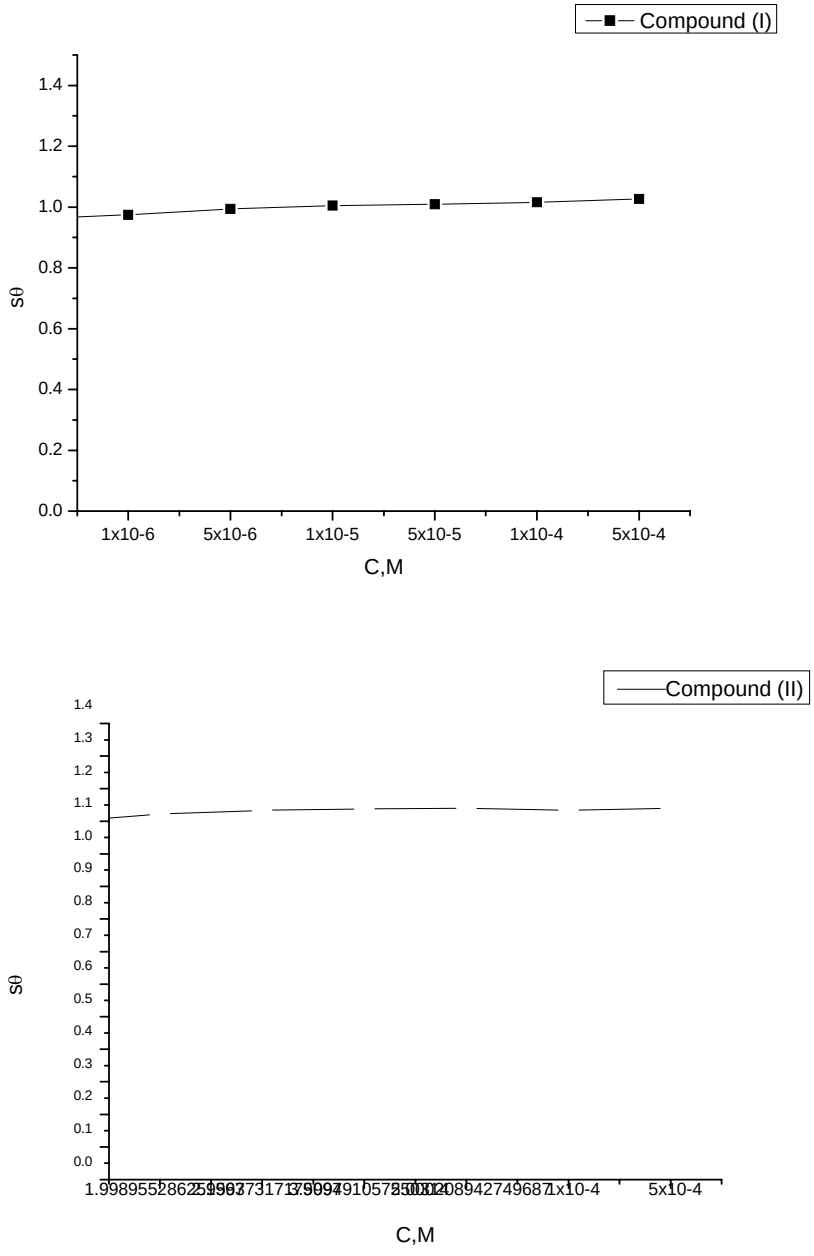

Fig(3.10): Plots of synergism parameter (S_θ) versus concentrations of investigated compounds for the corrosion of aluminum in 1M HCl with addition of $1x10^{-2}$M KI at 30 ^oC

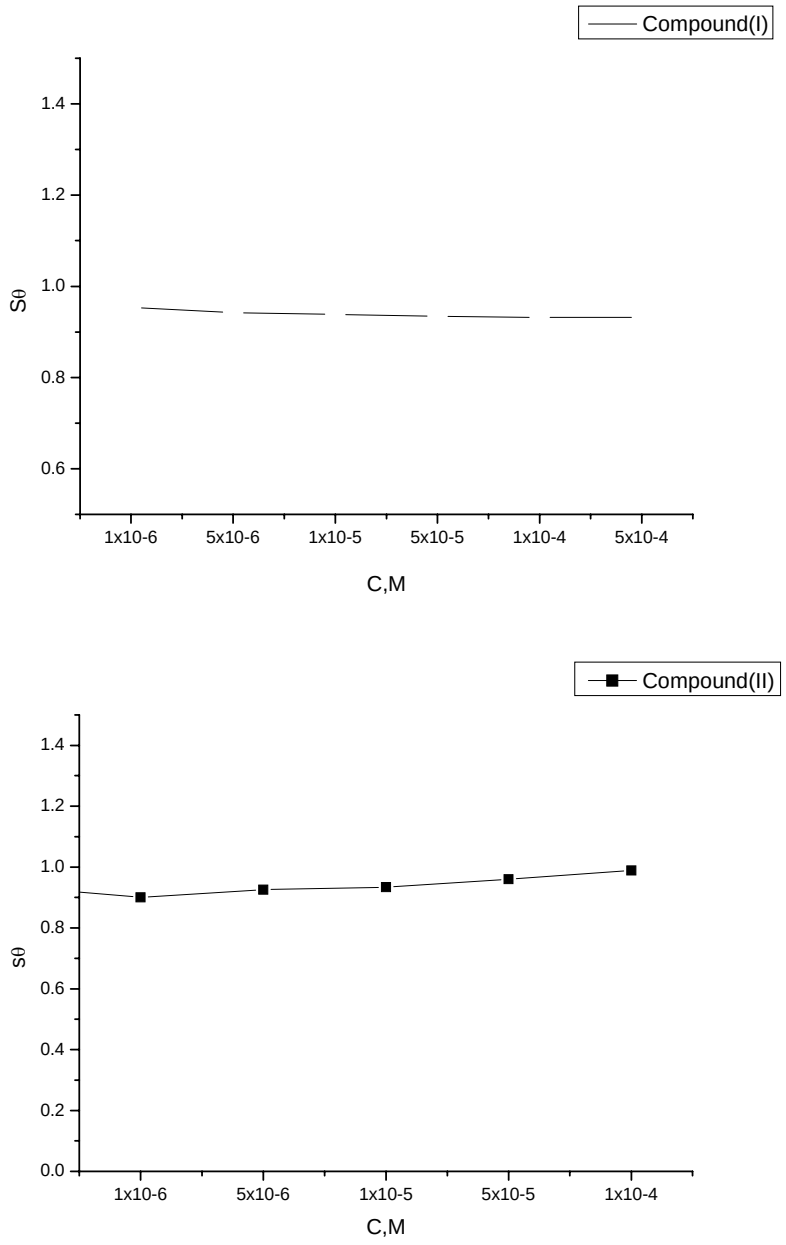

Fig(3.11): Plots of synergism parameter (S_θ) versus concentrations of investigated compounds for the corrosion of aluminum in 1M HCl with addition of $1x10^{-2}$ M KSCN at 30^oC.

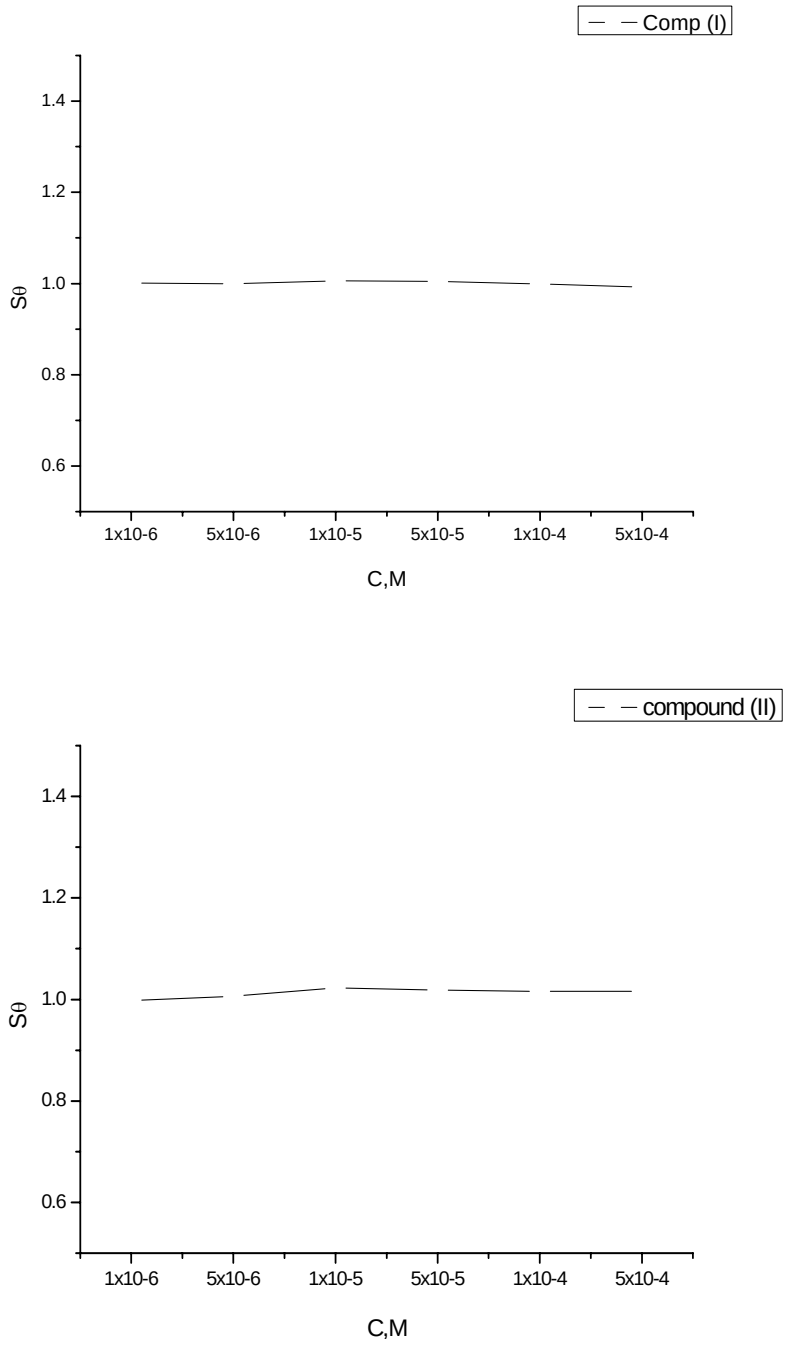

Fig(3.12): Plots of synergism parameter (S_θ) versus concentrations of investigated compounds for the corrosion of aluminum in 1M HCl with addition of $1x10^{-2}$M KBr at 30^oC

Table(3.5): Synergism parameter(S_θ) for different concentration of investigated compounds with addition of $1x10^{-2}$ M KI for the corrosion of aluminum in 1M HCl , after 120 min immersion and at 30 ^oC.

Concentration	Synergism parameter (S_θ)	
M	compound (I)	compound (II)
$1x10^{-6}$	1.007	0.920
$5x10^{-6}$	1.016	0.948
$1x10^{-5}$	1.022	0.958
$5x10^{-5}$	1.028	0.992
$1x10^{-4}$	1.102	1.007
$5x10^{-4}$	1.107	1.024

Table (3.6): Synergism parameter(S_θ) for different concentration of investigated compounds with addition of $1x10^{-2}$ M KSCN for the corrosion of aluminum in 1M HCl ,after 120 min immersion and at 30 ^oC

Concentration	**Synergism parameter(S_θ)**	
M	compound (I)	compound (II)
$1x10^{-6}$	1.008	0.900
$5x10^{-6}$	1.016	0.926
$1x10^{-5}$	1.019	0.934
$5x10^{-5}$	1.023	0.960
$1x10^{-4}$	1.033	0.989
$5x10^{-4}$	1.043	1.005

Table (3.7): Synergism parameter (S_θ) for different concentration of investigated compounds with addition of $1x10^{-2}$ M KBr for the corrosion of aluminum in 1M HCl after 120 min immersion and at 30 ^oC.

Concentration M	**Synergism parameter(S_θ)**	
	compound (I)	compound (II)
$1x10^{-6}$	0.972	0.893
$5x10^{-6}$	0.975	0.902
$1x10^{-5}$	1.005	0.926
$5x10^{-5}$	1.009	0.933
$1x10^{-4}$	1.016	0.960
$5x10^{-4}$	1.027	0.963

3.3-Adsorption Isotherm

Organic molecules as Phenazones inhibit the corrosion process by the adsorption on metal surface. Theoretically, the adsorption process can be regarded as a single substitutional process in which an inhibitor molecule, I, in the aqueous phase substitutes an "x" adsorbed on the metal surface vis,

$$I_{(aq)} + xH_2O_{(sur)} \longrightarrow I_{(sur)} + xH_2O_{(aq)} \quad (3.2)$$

where x is known as the size ratio and simply equals the number of adsorbed water molecules replaced by a single inhibitor molecule. The adsorption depends on the structure of the inhibitor, the type of the metal and the nature of its surface, the nature of the corrosion medium and its pH value, the temperature and the electrochemical potential of the metal-solution interface. Also, the adsorption provides information about the interaction among the adsorbed molecules themselves as well as their interaction with the metal surface. Actually an adsorbed molecule may make the surface more difficult or less difficult for another molecule to become attached to a neighboring site and multilayer adsorption may take place. There may be more or less than one inhibitor molecule per surface site. Finally, various surface sites could have varying degrees of activation. For these reasons a number of mathematical adsorption isotherm expressions have been developed to take into consideration some of non-ideal effects.

Adsorption isotherm equations are generally of the form:

$$f(\theta, x) \exp(-a, \theta) = KC \quad (3.3)$$

where f (θ, x) is the configurational factor that depends essentially on the physical model and assumptions underlying the derivation of the isotherm is a molecular interaction parameter depending upon molecular interactions in the adsorption layer and the degree of heterogeneity of the surface. All adsorption expressions include the equilibrium constant of the adsorption process, K which is related to the standard free energy of adsorption ($\Delta G°_{ads.}$) by:

$$K = 1/55.5 \exp(-\Delta G^{\circ}_{ads.} / RT) \quad (3.4)$$

where R is the universal gas constant and T is the absolute temperature.

A number of mathematical relationships for the adsorption isotherms have been suggested to fit the experiment data of the present work. The Temkin adsorption isotherm is given by the following equation:

$$a\,\theta = \ln KC \quad (3.5)$$

where K is the equilibrium constant of the adsorption reaction, C is the inhibitor concentration in the bulk of the solution and a is the inter action parameter. The surface coverage, i.e., the fraction of the surface covered by the inhibitor molecules, θ was calculated from the following known equation (2.12).

Plots of θ vs.log C (Temkin adsorption plots) for adsorption of investigated compounds on the surface of aluminum and in 1M HCl acid at 25^0C are shown in Fig. (3.13). The data gave linear shape indicating that Temkin's isotherm is valid for these systems.

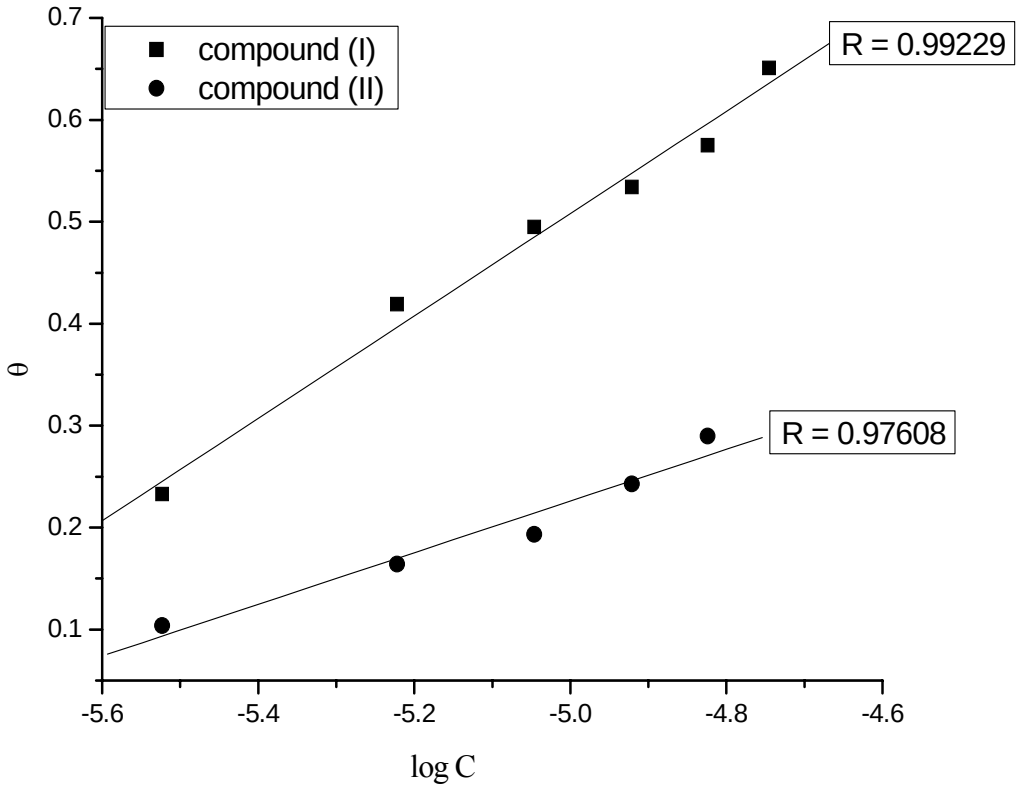

Fig (3.13): θ vs.log C for the corrosion of aluminum in 1M HCl in the presence of different concentrations of investigated compounds to Temkin adsorption isotherm at 30°C.

SECTION (B)

STUDYING THE CORROSION BEHAVIOR OF ALUMINUM AND ALUMINUM-SILICON ALLOY BY THE ELECTROCHEMICAL TECHNIQUES

Electrochemical techniques are based on current and potential measurements. It is generally accepted that the inhibitor molecule inhibits corrosion by adsorbing at the metal/solution interface. However, the modes of adsorption are dependant upon the followings:

1- Chemical structures of the adsorbate molecule.
2- Chemical composition of the solution.
3- Nature of the metal surface.
4- Electrochemical potential at the interface.

One or a combination of the three principle types of adsorption [136]:
π-bond, electrostatics or chemisorptions.

When designing inhibitors, all of theories are in common agreement that adsorption phenomena involves either:

1- proton acceptor (cathodic site absorber), material in this group accepts the hydrogen ion or proton and migrates to the cathode.
2- Electron acceptor (anodic site absorber), inhibitor function is due to its ability to accept electrons. Passivator's type and inhibitors are found in this group or both.
3- ambiodic (adsorb at anodic and cathodic sites). It has been generally accepted that group contributions vary considerably from molecule to molecule . The overall molecular charge in given position depends heavily upon the actual site and geometry of the neighboring group. Utilization of these concepts permits the systematic construction and increasing inhibition efficiency of organic molecule.

3.4-Potentiodynamic polarization method.

Potentiodynamic polarization method is useful in this study because they give more information about the corrosion mechanism and the factors affect the corrosion process and inhibition behavior of the additive compounds. This is achieved by measuring the potential- current characteristics of the metal/ solution system.

In potentiodynamic polarization method the aluminum electrode was under potential control and the corresponding current was allowed to vary. Potentiodynamic polarization curves of aluminum and aluminum- silicon in 1M HCl in the absence and presence of different concentrations of the investigated compounds at 25^{o}C are illustrated in Figs. (3.14-3.17).

For the potentiodynamic measurements the degree of surface coverage (θ) and the inhibition efficiency (%IE) were calculated from equations (2.11 and 2.3) respectively.

3.4.1- Poteniodynamic polarization

The numerical values of the variation of corrosion current density (i_{corr}) corrosion potential (E_{corr}) Tafel slopes (β_a and β_c), degree of surface coverage (θ) and inhibition efficiency (%IE) with the concentrations of different compounds are given in Tables (3.8-3.9).

This indicates that: It can see from the experimental results that these investigated compounds decrease i_{corr} significantly at all the studied concentrations. The presence of these compounds resulted in a slightly shift of corrosion potential towards the active direction in comparison to the result obtained in the absence of the inhibitor Both the anodic and cathodic current densities were decreased .

Fig.(3.18) shows the plot of θ vs log C for the investigated compounds .The linear relationship indicates the validy of Temkin adsorption isotherm for these investigated compounds. This is similar in case of weight loss method.

Also; Fig.(3.19) shows the validity of the Temkin adsorption isotherm for aluminum-silicon alloy.

This result shows that the addition of investigated compounds reduced anodic dissolution and also retards the hydrogen evolution reaction.

In the presence of investigated compounds, the change of the corrosion potential (E_{corr}) is negliable, therefor, these compounds arranged as amixed-type inhibitors in HCl solution and its inhibition on Al and Al-Si alloy is caused by geometric blocking effect [137].

The order of decreasing inhibition efficiency of the investigated compounds is as follows:

compound (I) > compound (II)

This is also in agreement with the observed order of corrosion inhibition by the weight loss method.

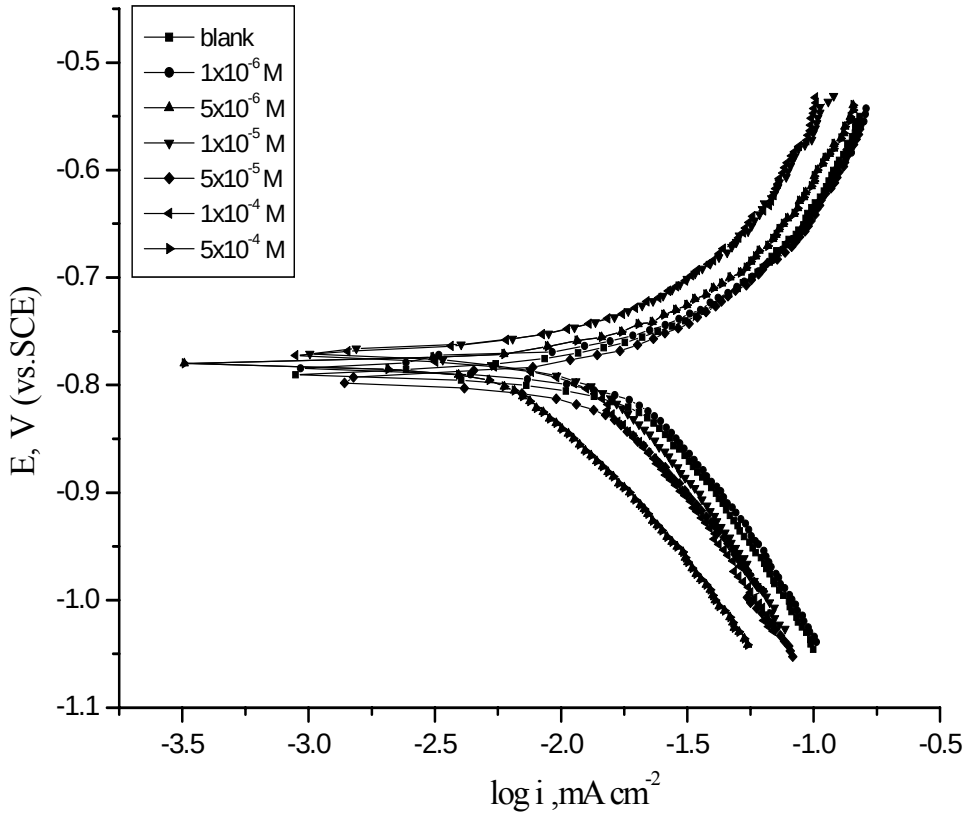

Fig.(3.14): Potentiodynamic polarization curves for the corrosion of aluminum in 1M HCl in the absence and presence of different concentrations of compound (I) at 25 ^{o}C

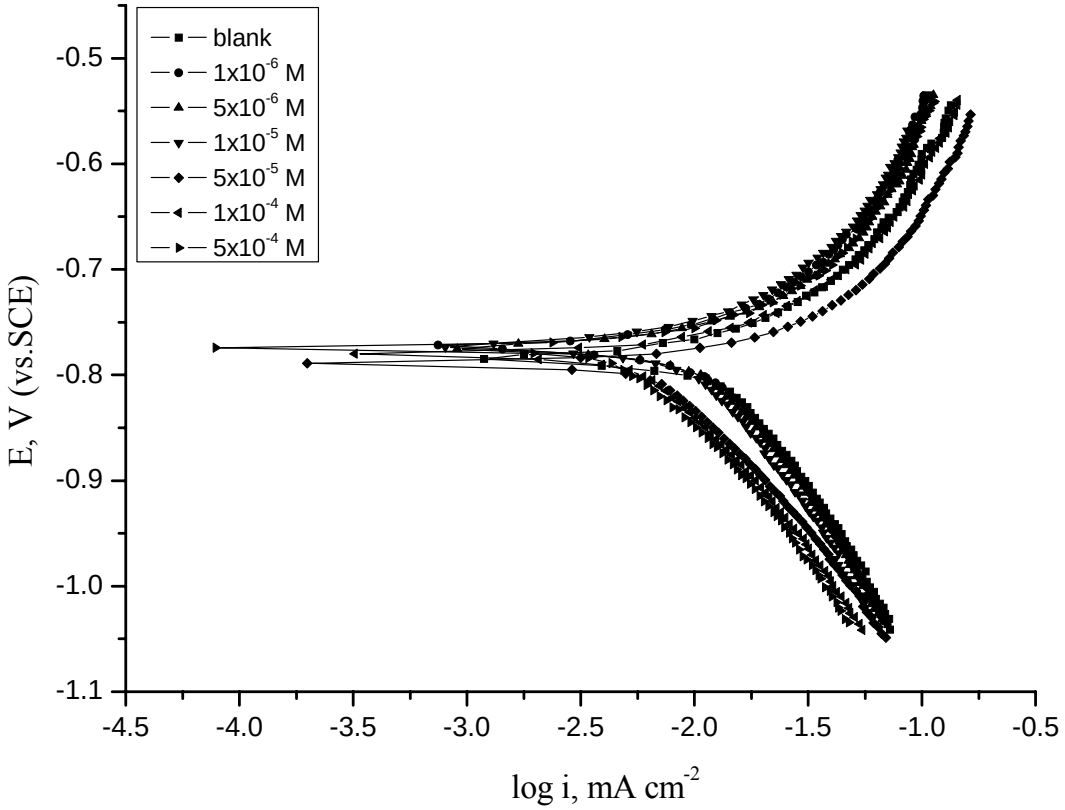

Fig.(3.15): Potentiodynamic polarization curves for the corrosion aluminum in 1 M HCl in the absence and presence of different concentrations of compound (II) at 25 ^{o}C.

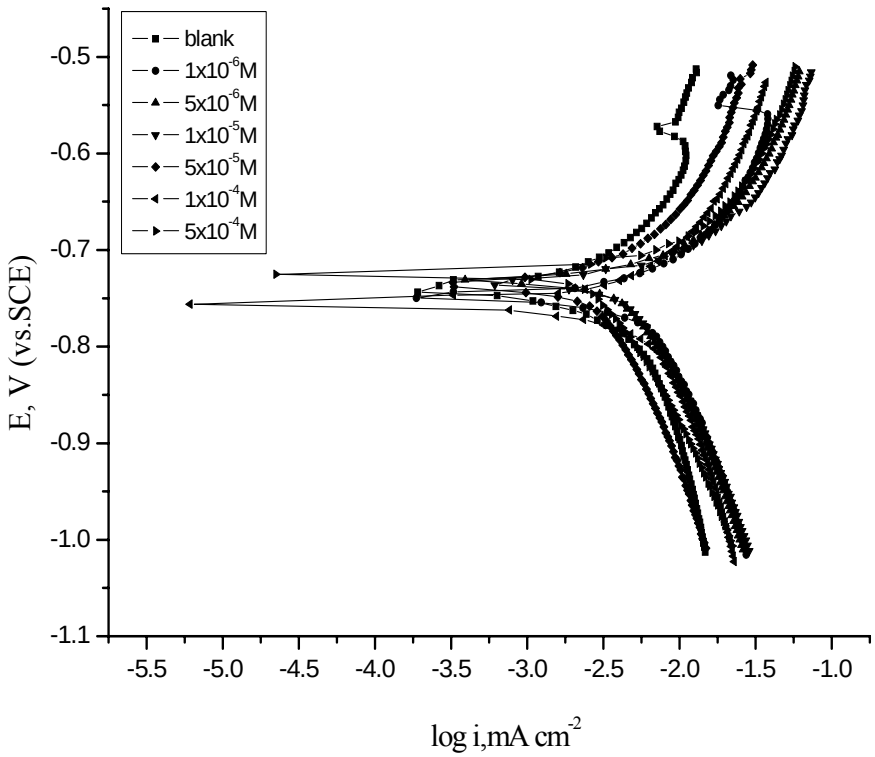

Fig. (3.16): Potentiodynamic polarization curves for the corrosion of aluminum - silicon in 1 M HCl in the absence and presence of different concentrations of compound (I) at 25 ^{o}C

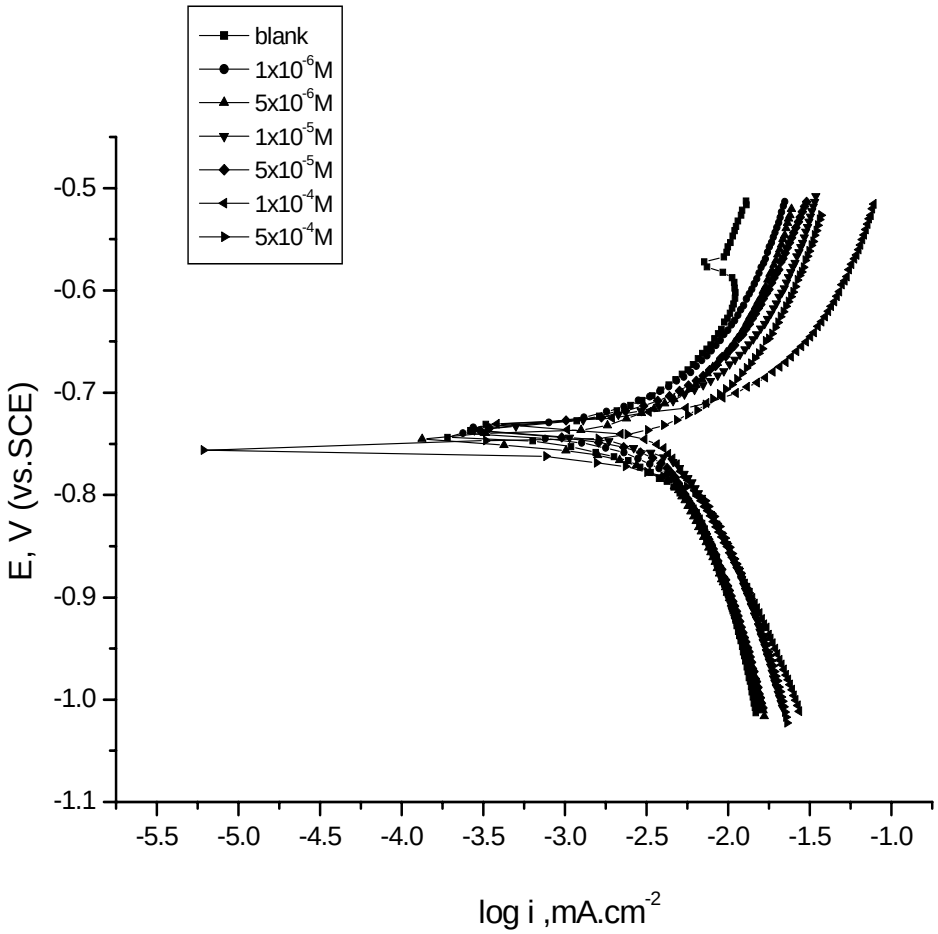

Fig(3.17):Potentiodynamic polarization curves for the corrosion of aluminum-silicon in 1 M HCl in the absence and presence of different concentrations of compound (II) at 25 ^{o}C

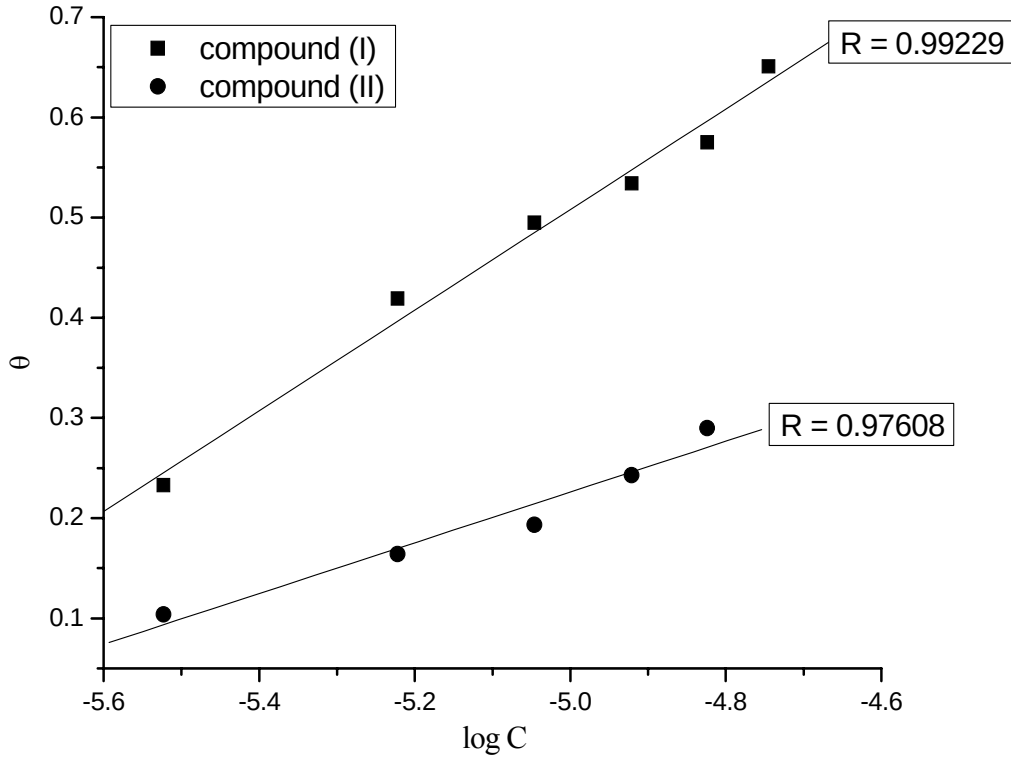

Fig (3:18): θ vs.log C for the corrosion of aluminum in 1M HCl in the presence of differe
concentrations of investigated compounds to Temkin adsorption isotherm at 2

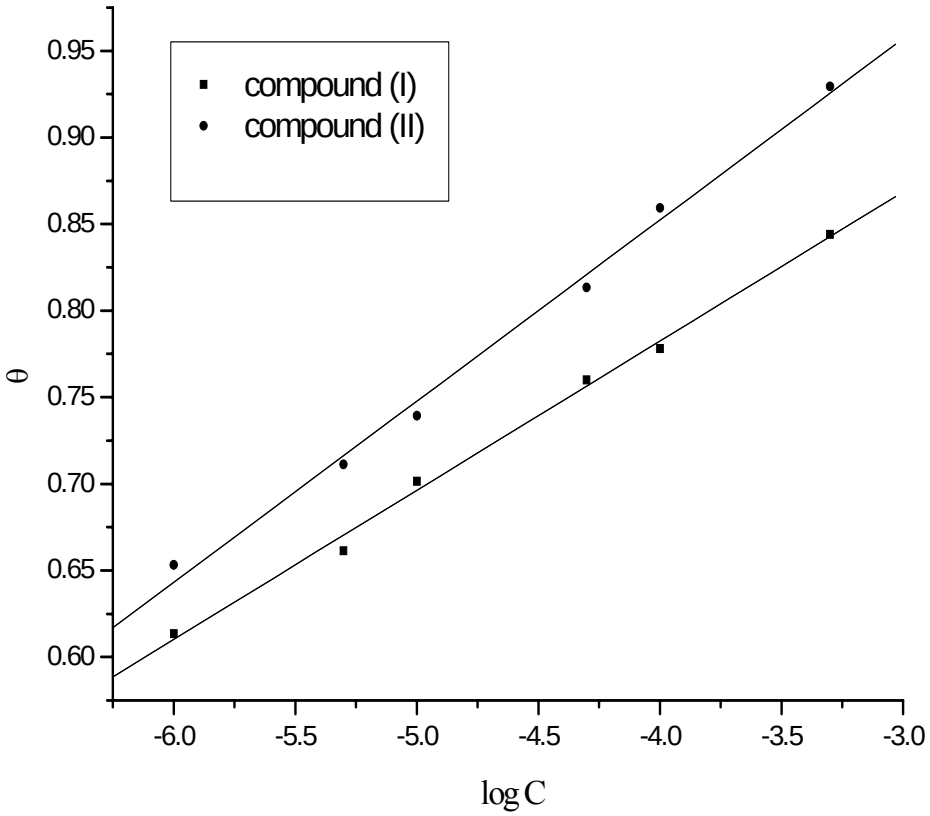

Fig (3.19): θ vs.log C for the corrosion of aluminum-silicon in 1M HCl in the presence of different concentrations of investigated compounds to Temkin adsorption isotherm at 25 °C.

Table (3.8): The effect of concentration of compound (I) on the free corrosion potential (E_{corr}) , corrosion current density (i_{corr}),Tafel slopes (β_a, β_c),inhibition efficiency (IE%), degree of surface coverage (θ) and corrosion rate (C.R.) for the corrosion of aluminum in 1M HCl at 25° C.

[Inh.], M	$-E_{corr}$, mV	i_{corr}, mA cm^{-2}	β_c, mV dec^{-1}	β_a, mV dec^{-1}	R_p Ω cm^2	Corrosion Rate mm/Year	Θ	IE%	
								I_{corr}	R_p
0	799	155	350	٦٦٤	1.998	1.68	0.0	0.0	0.0
$1x10^{-6}$	774	97	٢٨٨	635	2.950	1.537	0.377	37.7	32.3
$5x10^{-6}$	٧٦٧	96	٣١٠	640	3.233	1.505	0.382	38.2	38.3
$1x10^{-5}$	٧٥٨	82	312	646	3.784	1.434	0.472	47.2	47.2
$5x10^{-5}$	٧٥٣	71	330	650	4.021	1.413	0.545	54.5	50.3
$1X10^{-4}$	٧٢٤	28	337	652	11.522	1.385	0.822	82.2	82.7
$5x10^{-4}$	٧١١	23	343	659	15.263	1.224	٠.868	86.8	86.9

Table(3.9): The effect of concentration of compound (II) on the free corrosion potential (E_{corr}) ,corrosion current density (i_{corr}),Tafel slopes (β_a, β_c), inhibition efficiency (IE%), degree of surface coverage (θ) and corrosion rate (C.R) for the corrosion of aluminum in 1M HCl at 25°C.

[Inh.], M	$-E_{corr}$, mV	i_{corr}, mA cm^{-2}	β_c, mV dec^{-1}	β_a, mV dec^{-1}	R_p Ω cm^2	Corrosion Rate mm/Year	Θ	IE%	
								I_{corr}	R_p
0	799	155	350	٦٦٤	1.998	1.68	0	0.0	0.0
$1x10^{-6}$	٧٩٨	117	289	611	2.448	1.583	0.245	24.5	22.5
$5x10^{-6}$	796	114	307	619	2.688	1.492	0.265	26.5	25.7
$1x10^{-5}$	٧٩٦	100	312	634	3.104	1.089	0.354	35.4	35.6
$5x10^{-5}$	٧٩١	95	330	644	4.052	1.011	0.386	38.6	50.7
$1x10^{-4}$	781	49	327	653	7.635	0.945	0.745	74.5	73.8
$5x10^{-4}$	6٧7	27	345	658	11.542	0.904	٠.828	82.8	82.6

Table(3.10): The effect of concentration of compound (I) on the free corrosion potential (E_{corr}), corrosion current density (i_{corr}),Tafel slopes (β_a, β_c), inhibition efficiency (IE%), degree of surface coverage (θ) and corrosion rate (C.R) for the corrosion of aluminum- silicon alloy in 1M HCl at 25 ^{o}C.

[Inh.], M	$-E_{corr}$, mV	i_{corr}, mA cm^{-2}	β_c, mV dec^{-1}	β_a, mV dec^{-1}	R_p Ω cm^2	Corrosion Rate mm/Year	Θ	IE%	
								I_{corr}	R_p
0	730	91	310	٦٢٤	8.863	9.9328	0.0	0.0	0.0
$1x10^{-6}$	717	72	٢٨٠	599	11.141	3.3647	0.208	20.8	20.5
$5x10^{-6}$	712	29	٢٩٠	612	26.954	3.2905	0.683	68.3	67.0
$1x10^{-5}$	703	25	٢٩٤	616	32.347	3.1527	0.726	72.6	72.5
$5x10^{-5}$	٦٩٥	19	٢٩٦	619	41.454	1.8877	0.791	79.1	78.6
$1x10^{-4}$	٦٨٨	18	٣٠٠	620	45.753	1.5572	0.802	80.2	80.6
$5x10^{-4}$	٦٥٨	15	٣٠٧	622	49.256	1.4918	0.835	83.5	82.0

Table(3.11): The effect of concentration of compound (II) on the free corrosion potential (E_{corr}) ,corrosion current density (i_{corr}),Tafel slopes (β_a,β_c),inhibition efficiency (IE%), degree of surface coverage (θ) and corrosion rate (C.R) for the corrosion of aluminum- silicon alloy in 1M HCl at 25 ^{o}C.

[Inh.], M	$-E_{corr}$, mV	i_{corr}, mA cm^{-2}	β_c, mV dec^{-1}	β_a, mV dec^{-1}	R_p Ω cm^2	Corrosion Rate mm/Year	Θ	IE%	
								I_{corr}	R_p
0	٧٣٠	91	310	٦٢٤	8.863	9.9328	0.0	0.0	0.0
$1x10^{-6}$	٧٢٦	38	٢٨١	٦٠١	22.961	5.8603	0.614	61.4	61.3
$5x10^{-6}$	715	31	٢٩٢	٦٠٩	26.145	4.12635	0.661	66.1	66.0
$1x10^{-5}$	702	24	٢٩٤	٦١٤	33.799	3.631	0.737	73.7	73.7
$5x10^{-5}$	694	23	٢٩٨	619	34.959	2.3521	0.745	74.5	74.7
$1x10^{-4}$	690	20	٣٠١	620	41.286	1.07368	0.780	78.0	78.5
$5x10^{-4}$	682	18	٣٠٩	623	43.673	1.01232	0.802	80.2	79.7

3.٥- Effect of temperature and activation parameters on the inhibition process

The influence of temperature on the corrosion rate of aluminum and aluminum -silicon alloy in 1M HCl in the absence and presence of $1x10^{-5}$M of the investigated compounds was investigated by the potentiodynamic polarization technique in temperature range (25 to 40^{o}C).

Figs. (3.20-3.23) show the potentiodynamic polarization curves for the corrosion of aluminum and aluminum –silicon alloy in 1M HCl in the absence and presence of $1x10^{-5}$M of the used compounds at temperatures 25, 30, 35 and 40^{o}C.

Plots of logarithm of corrosion rate (log k), with reciprocal of absolute temperature (1/T) for aluminum and aluminum -silicon alloy in 1M HCl at $1x10^{-5}$M for the investigated compounds are shown in Fig. (3.24-3.25). As shown from this Figure, straight lines with slope $-E_a^*/ 2.303R$ and intercept of A were obtained according to Arrhenuis-type equation[138]

$$k = A \exp (- E_a^*/ RT) \quad (3.6)$$

where:

k is the corrosion rate, A is a constant depends on a metal type and electrolyte, E_a^* is the apparent activation energy, R is the universal gas constant and T is the absolute temperature.

Plots of log (corrosion rate/ T) vs. 1/ T for aluminum and aluminum-silicon alloy in 1M HCl at $1x10^{-5}$M for the investigated compounds are shown in Figs. (3.26 -3.27). As shown from this Figure, straight lines with slope of ($-\Delta H^*/ 2.303R$) and intercept of ($\log R/ Nh + \Delta S^*/ 2.303R$) were obtained according to transition state equation:

$$\text{Rate} = RT/ Nh \exp (\Delta S^*/ R) \exp (-\Delta H^*/ RT) \quad (3.7)$$

where:

h is Planck's constant, N is Avogadro's number, ΔH^* is the activation enthalpy and ΔS^* is the activation entropy.

The calculated values of the apparent activation energy, E_a^*, activation enthalpies, ΔH^* and activation entropies, ΔS^* from aluminum and aluminum-silicon alloy are given in Tables (3.12-3.13). These values indicate that the presence of the additives increases the activation energy, E_a^* and the activation enthalpy, ΔH^* and decreases the activation entropy, ΔS^* for the corrosion process. The increase in the activation energy indicating a strong adsorption of the inhibitor molecules on aluminum pure or aluminum-silicon alloy surface and indicates the energy barrier caused by the adsorption of the additive molecules on aluminum and its alloy surface. The increase in the activation enthalpy (ΔH^*) in presence of the inhibitors implies that the addition of the inhibitors to the acid solution increases the height of the energy barrier of the corrosion reaction to an extent depends on the type and concentration of the present inhibitor. The entropy of activation (ΔS^*) in the blank and inhibited solutions is large and negative indicating that the activated complex represents association rather than dissociation step

The order of decreasing inhibition efficiency of the investigated compounds as gathered from the increase in E_a^* and ΔH^*_{ads} values and decrease in ΔS^*_{ads} is the higher inhibition efficiency for aluminum than in aluminum-silicon alloy due to the presence of silicon in the alloy

compound (I) > compound (II)

Aluminum > Aluminum -silicon

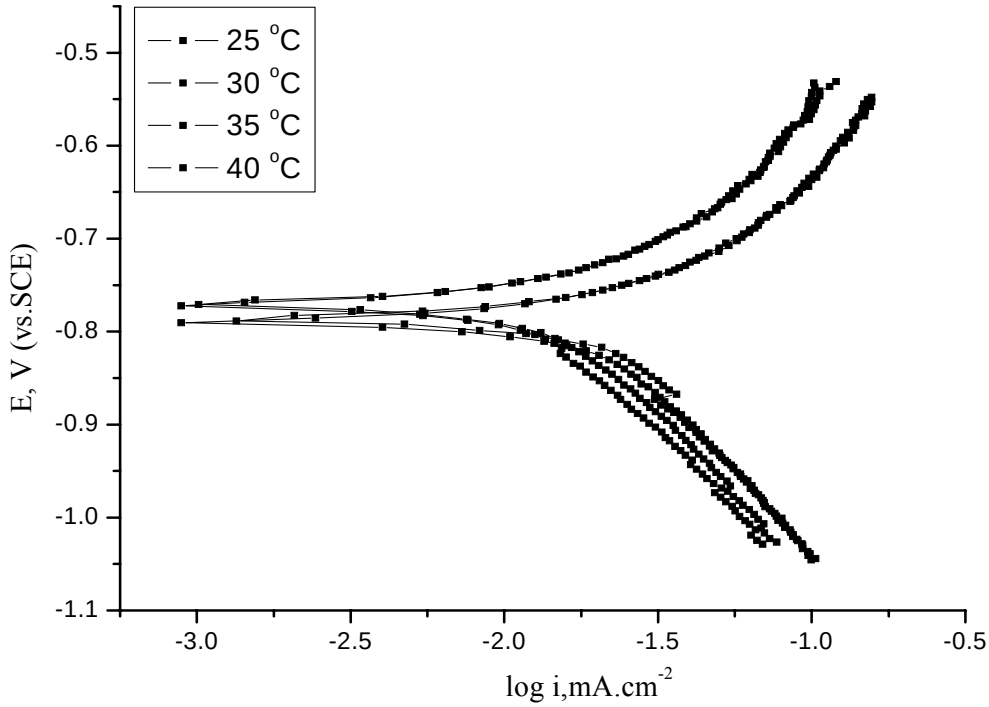

Fig.(3.20):Effect of temperature on potentiodynamic polarization curves for the corrosion of aluminum in 1M HCl in the presence of $1x10^{-5}$ M of compound (I).

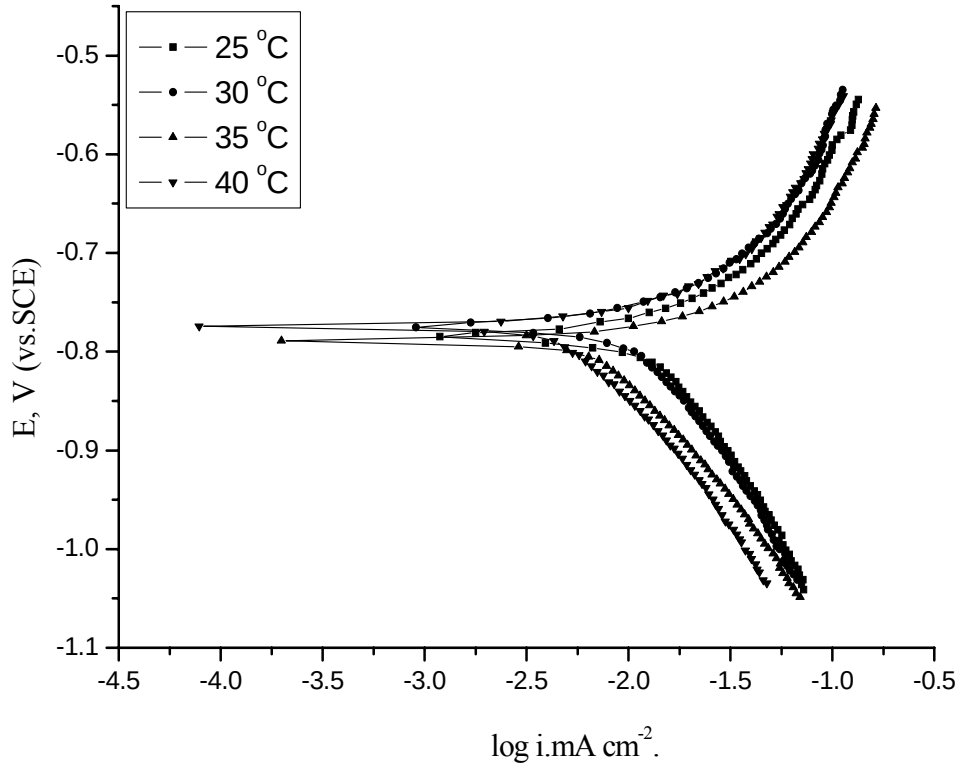

Fig.(3.21): Effect of temperature on potentiodynamic polarization curves for the corrosion of aluminum in 1 M HCl in the presence of $1x10^{-5}$ M of compound (II).

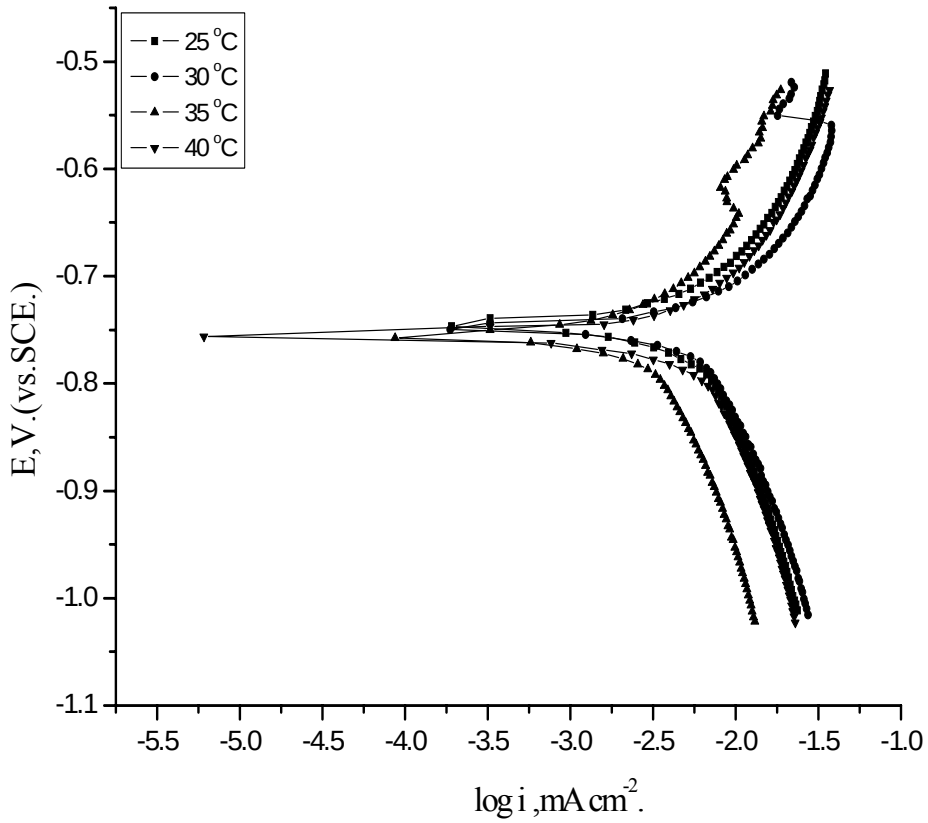

Fig.(3.22):Effect of temperature on potentiodynamic polarization curves for the corrosion of aluminum-silicon in 1 M HCl in the presence of $1x10^{-5}$ M of compound (I)

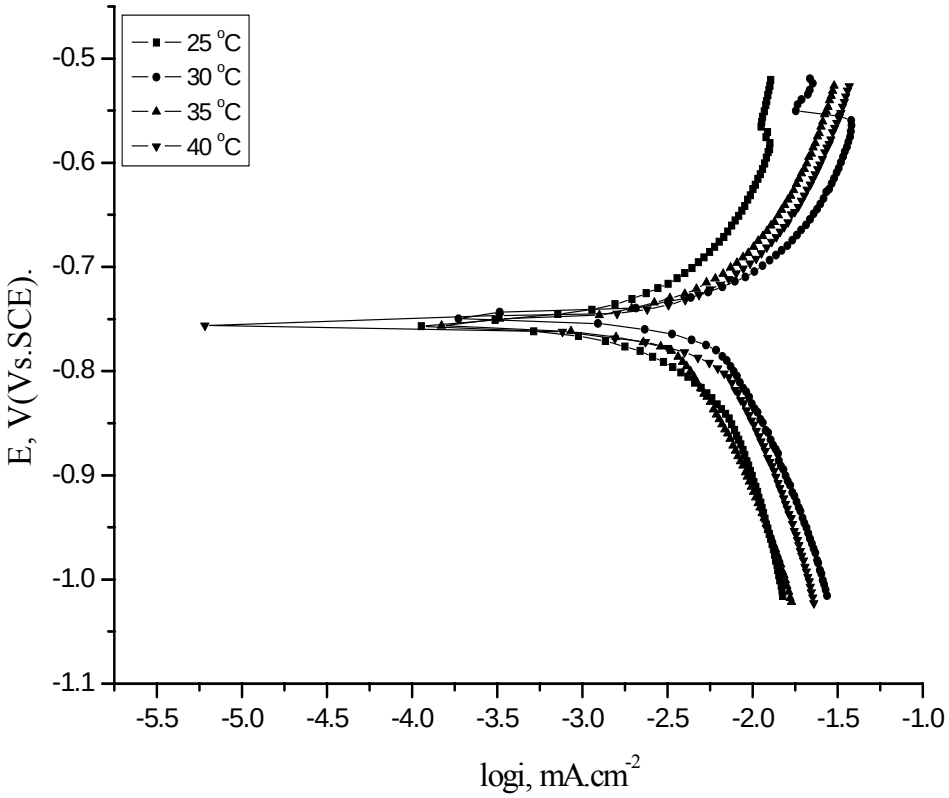

Fig.(3.23):Effect of temperature on potentiodynamic polarization curves for the corrosion of aluminum-silicon in 1 M HCl in the presence of $1x10^{-5}$ M of compound (II)

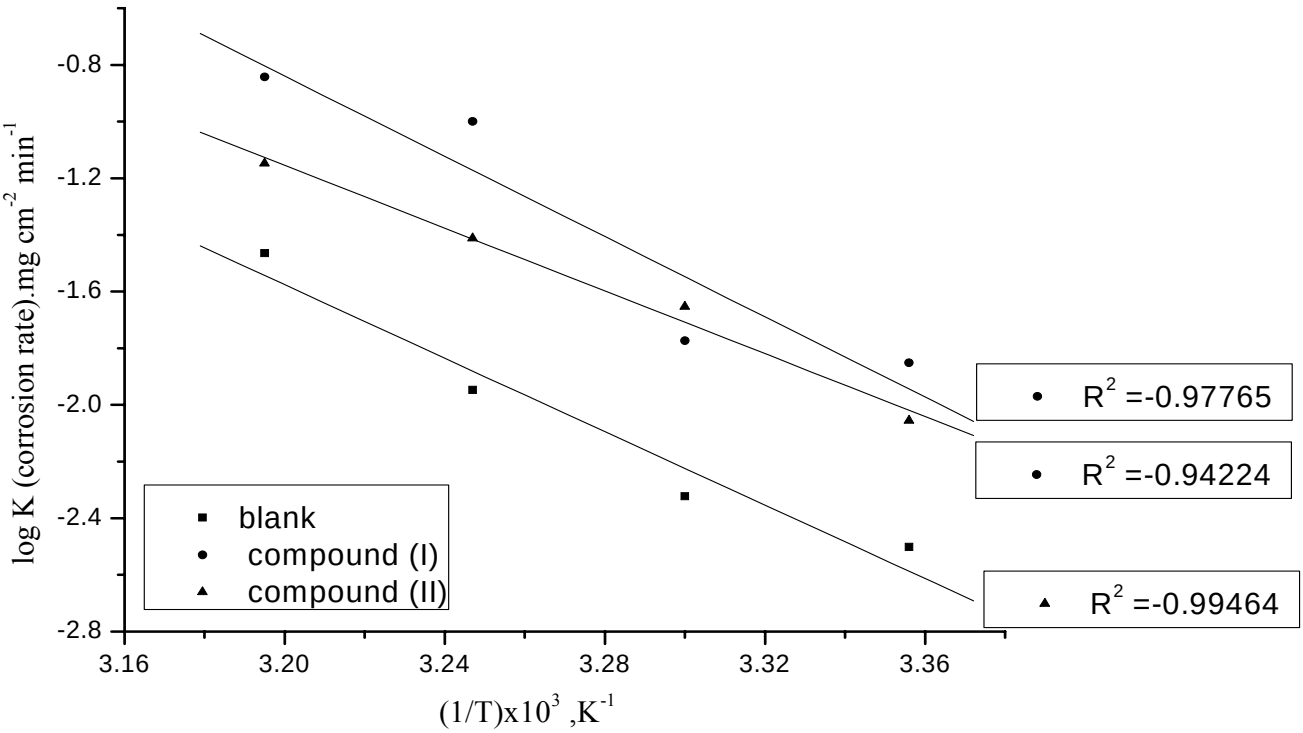

Fig.(3.24):log corrosion rate-1/T curves for the corrosion of aluminum in 1 M HCl at 1x10^{-5} M for the investigated compounds.

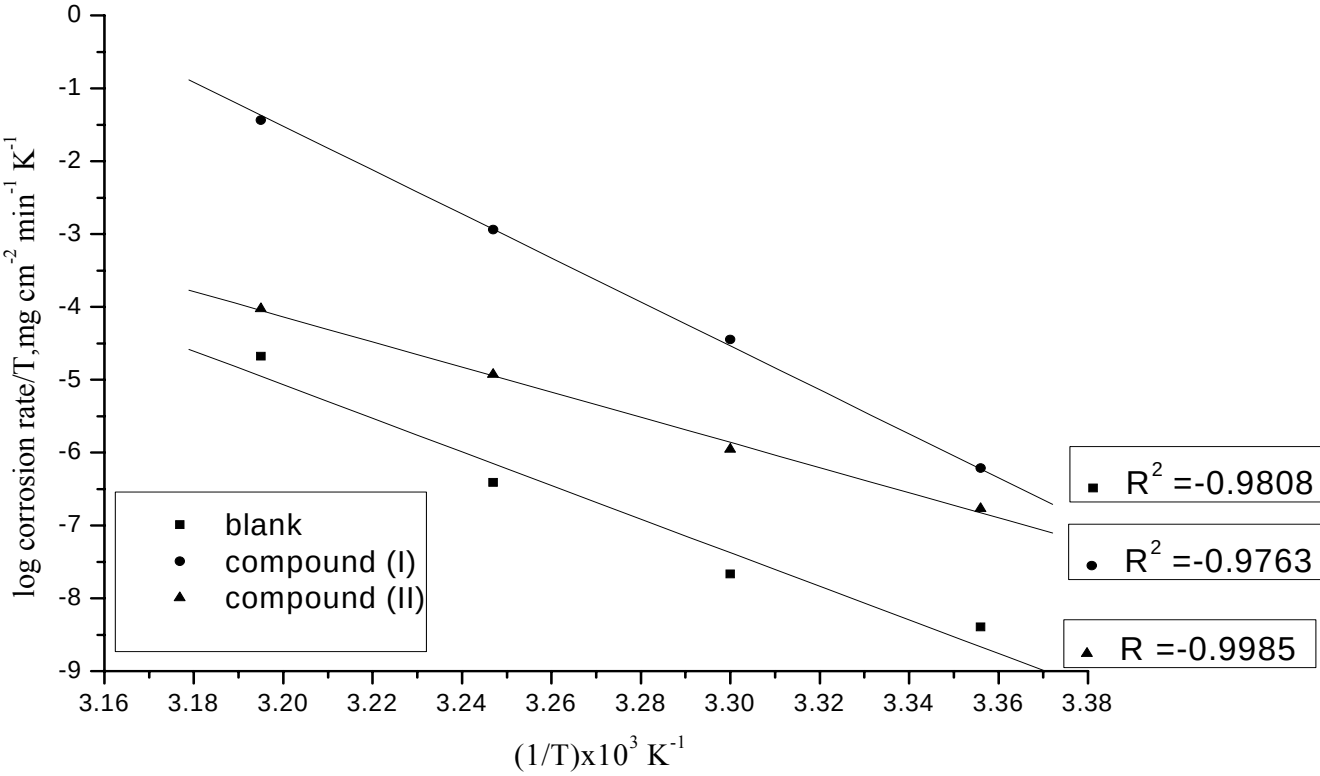

Fig.(3.25):log (corrosion rate/T)-(1/T)curves for the corrosion of aluminum in 1M HCl at 1x10^{-5} M for the investigated compounds.

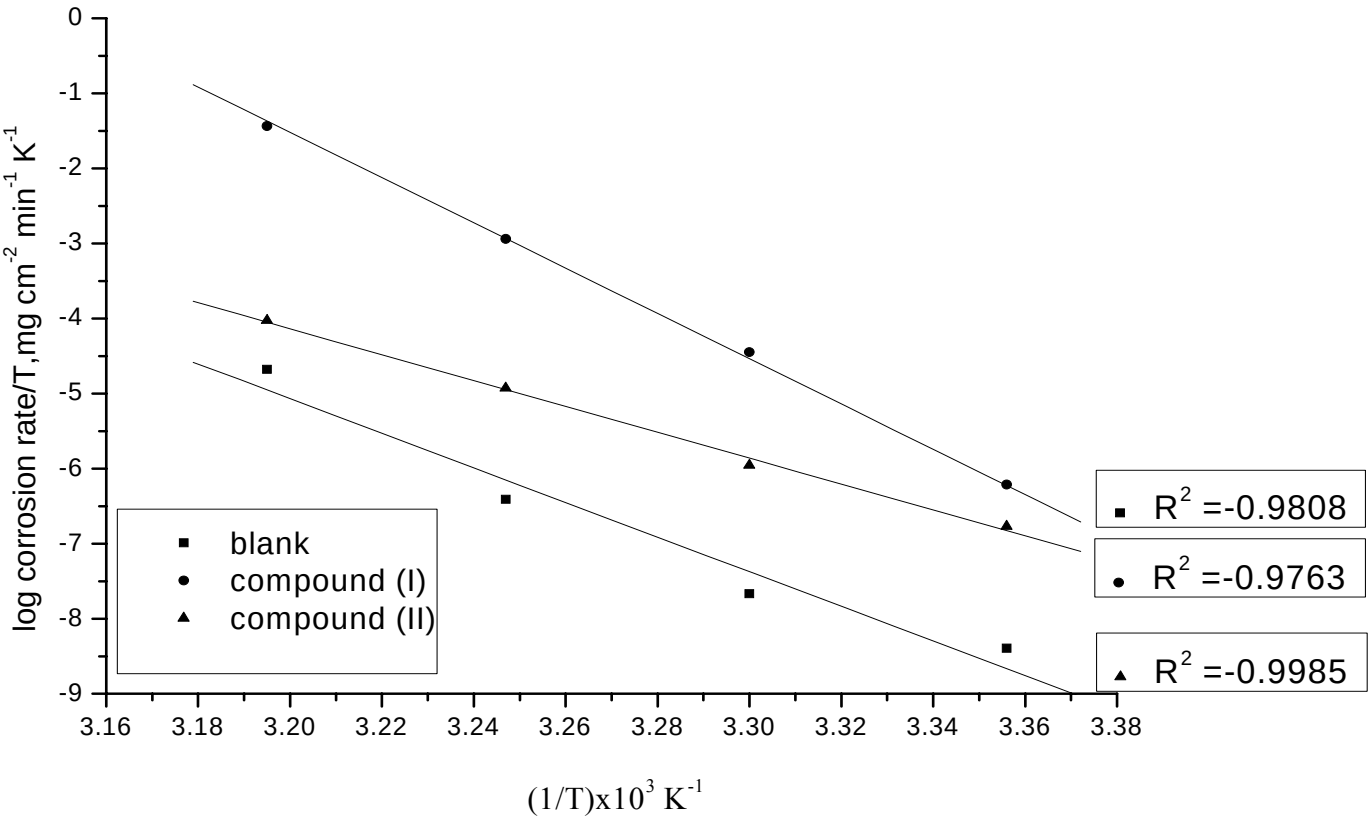

Fig.(3.26):log (corrosion rate/T)-(1/T)curves for the corrosion of aluminum-silicon alloy in 1M HCl at $5x10^{-5}$ M for the investigated compounds.

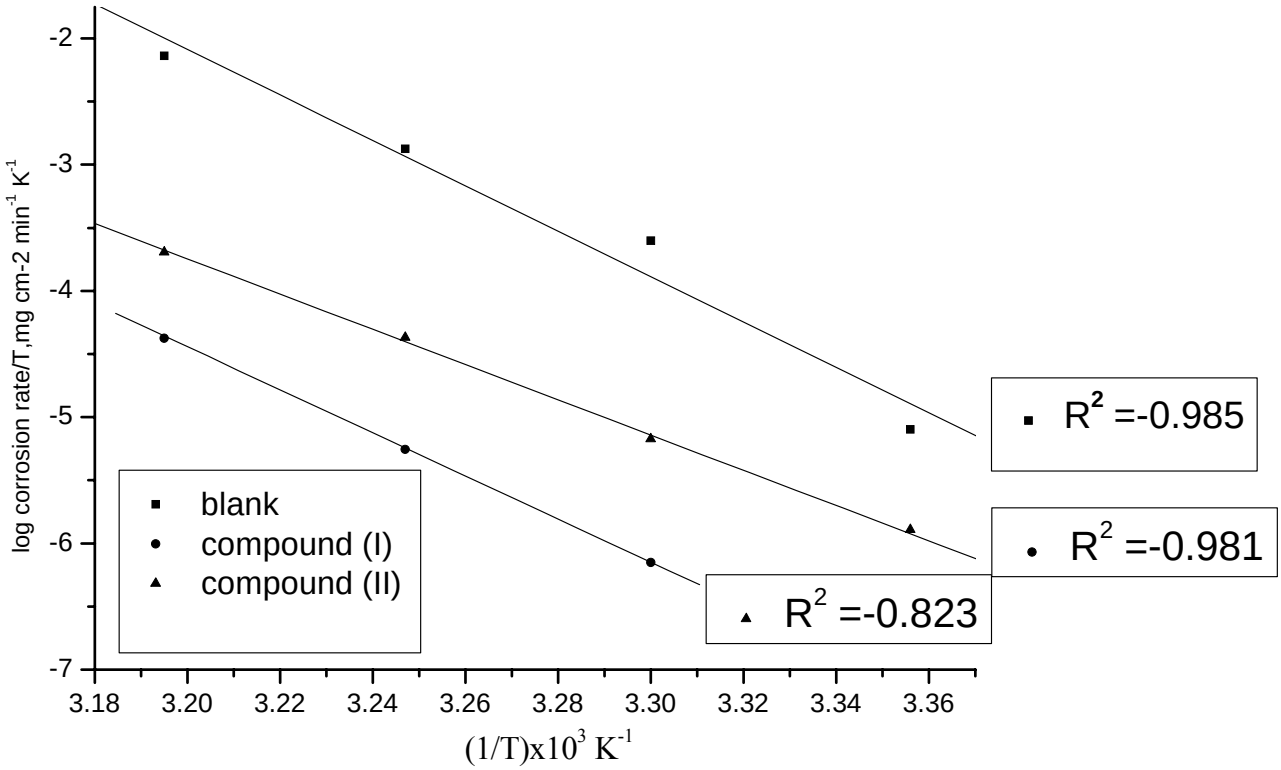

Fig.(3.27): log (corrosion rate/T)-(1/T)curves for the corrosion of aluminum-silicon alloy in 1 M HCl at $1x10^{-5}$ M for the investigated compounds.

Table (3:12) : Activation parameters of the corrosion of aluminum in 1M HCl at $1x10^{-5}$ M for the investigated compounds.

compound	E^*_a kJ mol^{-1}	ΔH^* kJ mol^{-1}	$-\Delta S^*$ $Jmol^{-1}$ k^{-1}
Free acid	10.6	33.0	234.6
Compound (I)	13.6	55.8	161.8
Compound (II)	12.4	44.2	112.8

Table (3:13): Activation parameters of the corrosion of aluminum– silicon alloy in 1 M HCl at $1x10^{-5}$ M for the investigated compounds.

compound	E^*_a kJ mol^{-1}	ΔH^* kJ mol^{-1}	$-\Delta S^*$ $Jmol^{-1}$ k^{-1}
Free acid	9.9	26.7	125.1
Compound (I)	17.1	34.4	110.5
Compound (II)	11.1	32.8	84.8

3.6- Electrochemical impedance spectroscopy (EIS)

The corrosion behavior of aluminum in1M HCl solution in the absence and presence of different concentrations of the investigated compounds was investigated by the EIS method at 25°C . Figs. (3.29-3.36) show the Nyquist and Bode plots for aluminum and aluminum -silicon in 1M HCl solution in the absence and presence of different concentrations of investigated compounds at 25°C. The obtained Nyquist impedance diagrams in most cases does not show perfect semicircle, generally attributed to the frequency dispersion [139] as a result of roughness and in homogenates of the electrode surface. The data reveal that, each impedance diagram consists of a large capacitive loop with low frequencies dispersion (inductive arc). This inductive arc is generally attributed to anodic adsorbed intermediates controlling the anodic process[140-142]. By following this , inductive arc was disregarded.

The impedance spectra of the different Nyquist plots (Fig.3.29-3.36) were analyzed by fitting the experimental data to a simple equivalent circuit model which shown in Fig. (3.28), which includes the solution resistance R_s and the double layer capacitance C_{dl} which is placed in parallel to the charge transfer resistance R_{ct}[143]

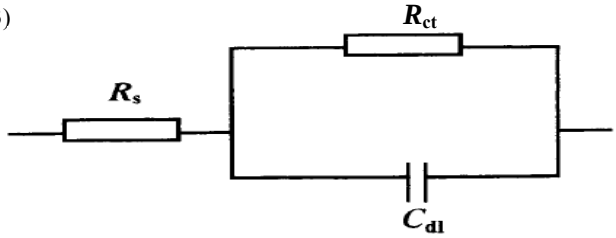

Fig.(3.28) The equivalent circuit model used to fit the experimental results.

In 1 M HCl with the presence of various concentrations of inhibitors, the impedance diagram shows the same trend (one capacitive loop), however, the diameter of this capacitive loop increases with increasing concentration.

The main parameters deduced from the analysis of Nyquist diagram are:

- The resistance of charge transfer R_{ct}(diameter of high frequency loop)

- The capacity of double layer C_{dl} which is defined as :

$$C_{dl} = \frac{1}{2\pi f_{max} R_{ct}} \quad (3.8)$$

where R_{ct} is the charge transfer resistance in the presence of inhibitor and f_{max} is maximum frequency.

The inhibition efficiency and the surface coverage (θ) obtained from the impedance measurements are defined by the following relations:

$$\%IE = \left(1 - \frac{R^{\circ}_{ct}}{R_{ct}}\right) x\,100 \quad (3.9)$$

$$\theta = \left(1 - \frac{R^{\circ}_{ct}}{R_{ct}}\right) \quad (3.10)$$

where R^{o}_{ct} and R_{ct} are the charge transfer resistance in the absence and presence of inhibitor, respectively. The associated with the diagrams impedance are given in Tables (3. 14-3. 16).

From the impedance data given in Tables (3. 14-3. 16), we conclude that:

- The value of R_{ct} increases with increase in the concentration of the inhibitors and this indicates an increase in the corrosion inhibition efficiency in acidic solution.
- As the impedance diagram obtained has a semicircle appearance, it shows that the corrosion of Al and Al-Si alloy is mainly controlled by a charge transfer process.
- The value of double layer capacitance decreases by increasing the inhibitor concentration. This is due to the adsorption of these compounds on the electrode surface of Al and Al-Si alloy leading to a film formation on the surface.
- The %IE obtained from EIS measurements are close to those deduced from polarization and weight loss methods.

The order of inhibition efficiency obtained from EIS measurements is as follows:

compound (I) > compound (II)

and Al > Al-Si alloy.

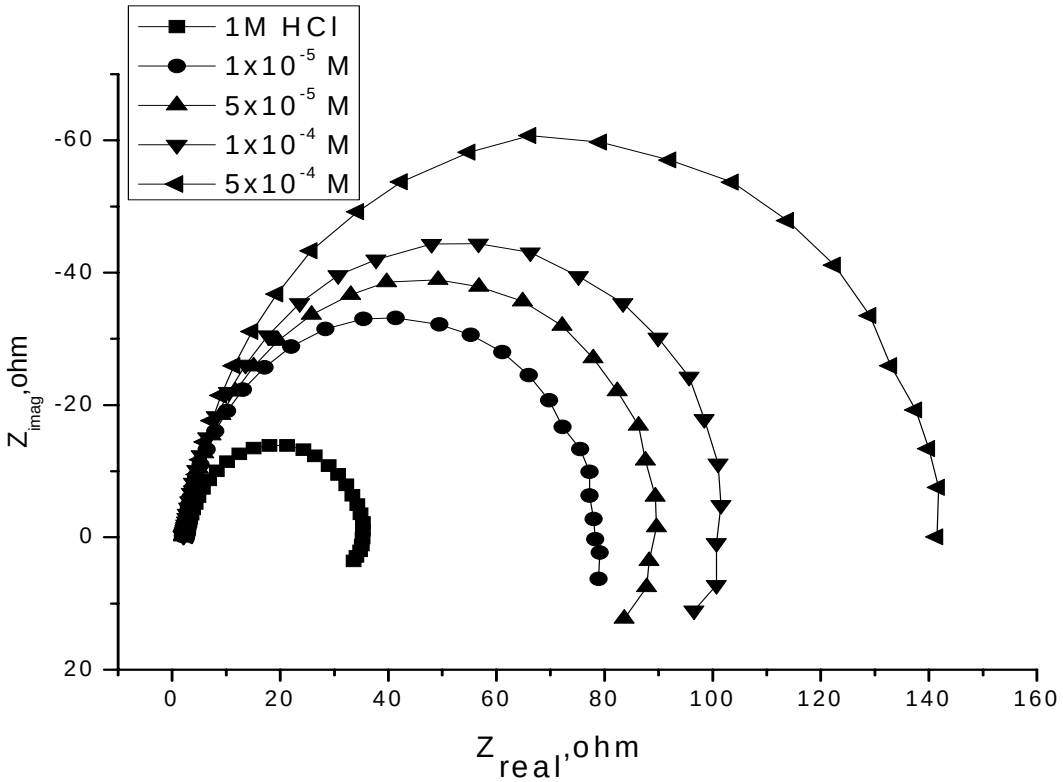

Fig(3.29): The Nyquist plots for aluminum in1 M HCl solution in the absence and presence of compound (I) at 25^{o}C.

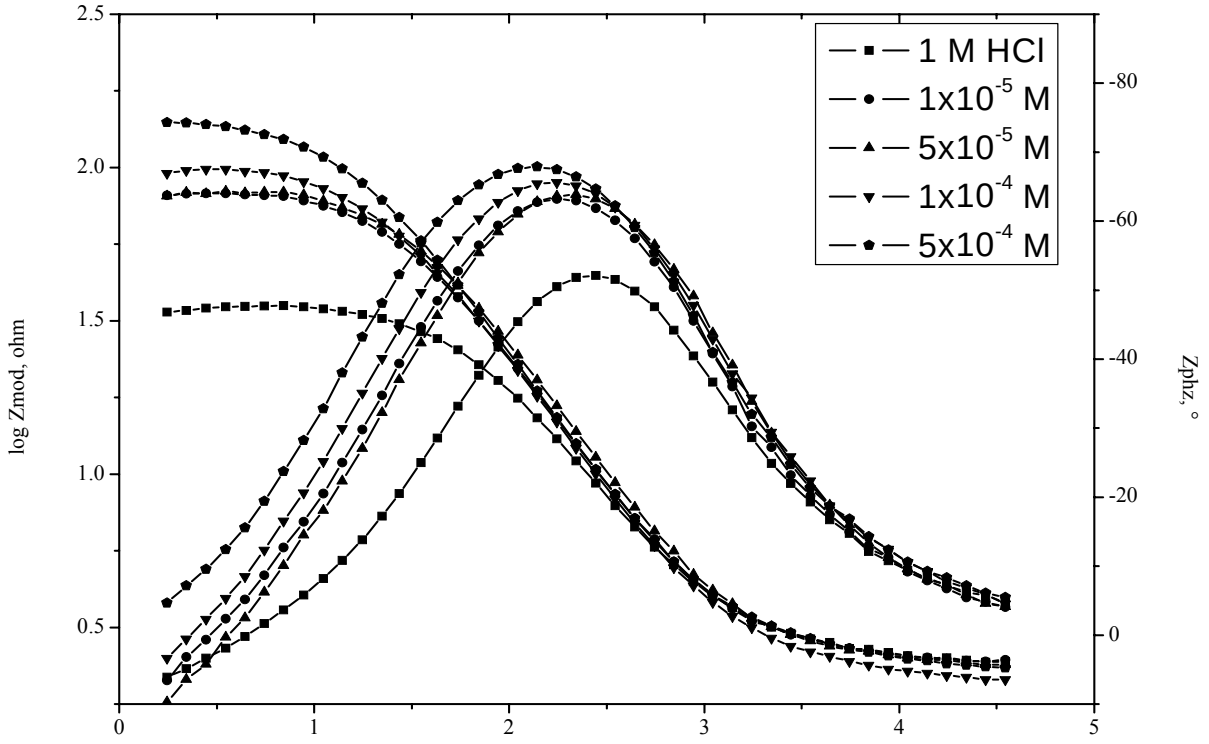

Fig(3:30): The Bode plots for aluminum in1 M HCl solution in the absence and presence of compound (I) at 25^{O}C.

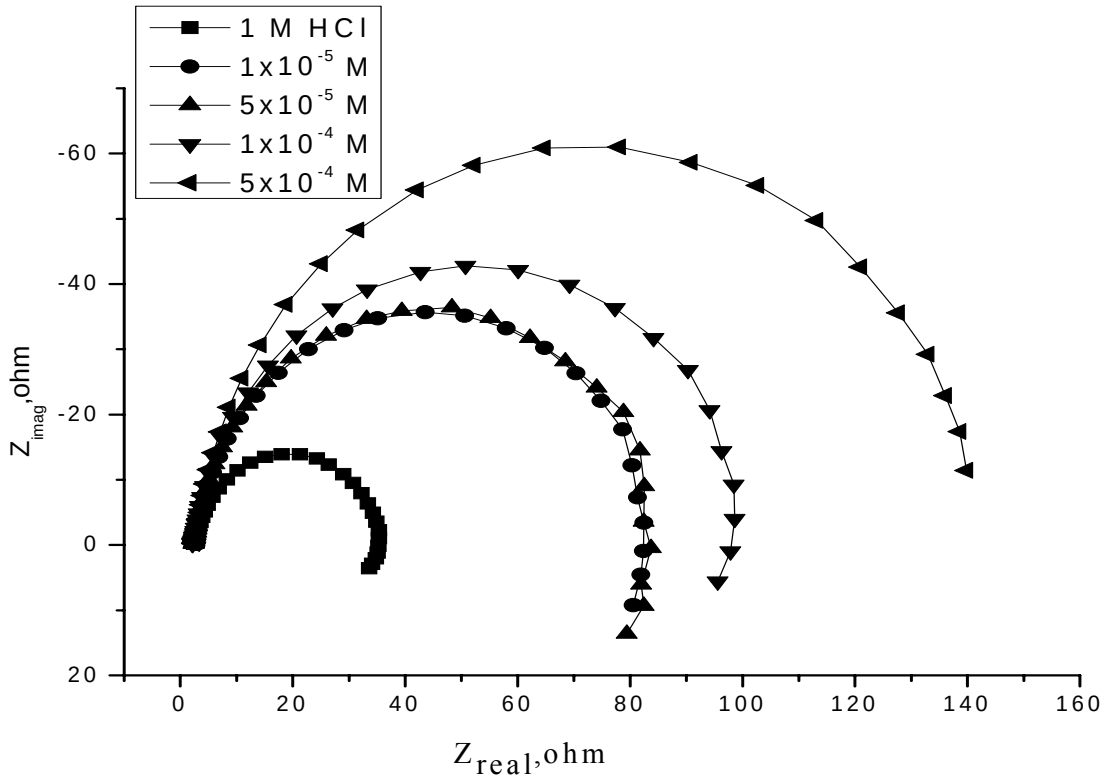

Fig(3.31): The Nyquist plots for aluminum in1 M HCl solution in ithe absence and presence of compound (II) at 25^{o}C.

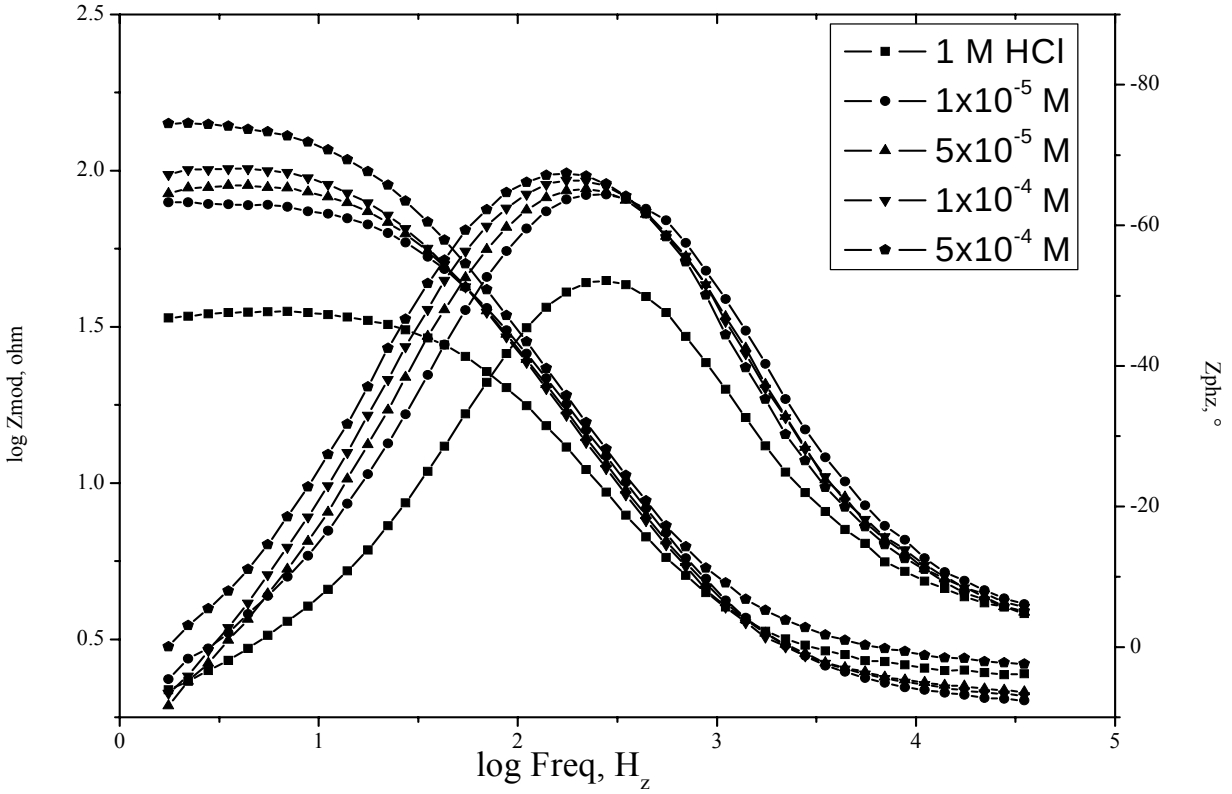

Fig(3.32): The Bode plots for aluminum in1 M HCl solution in the absence and presence of compound (II) at 25^{O}C.

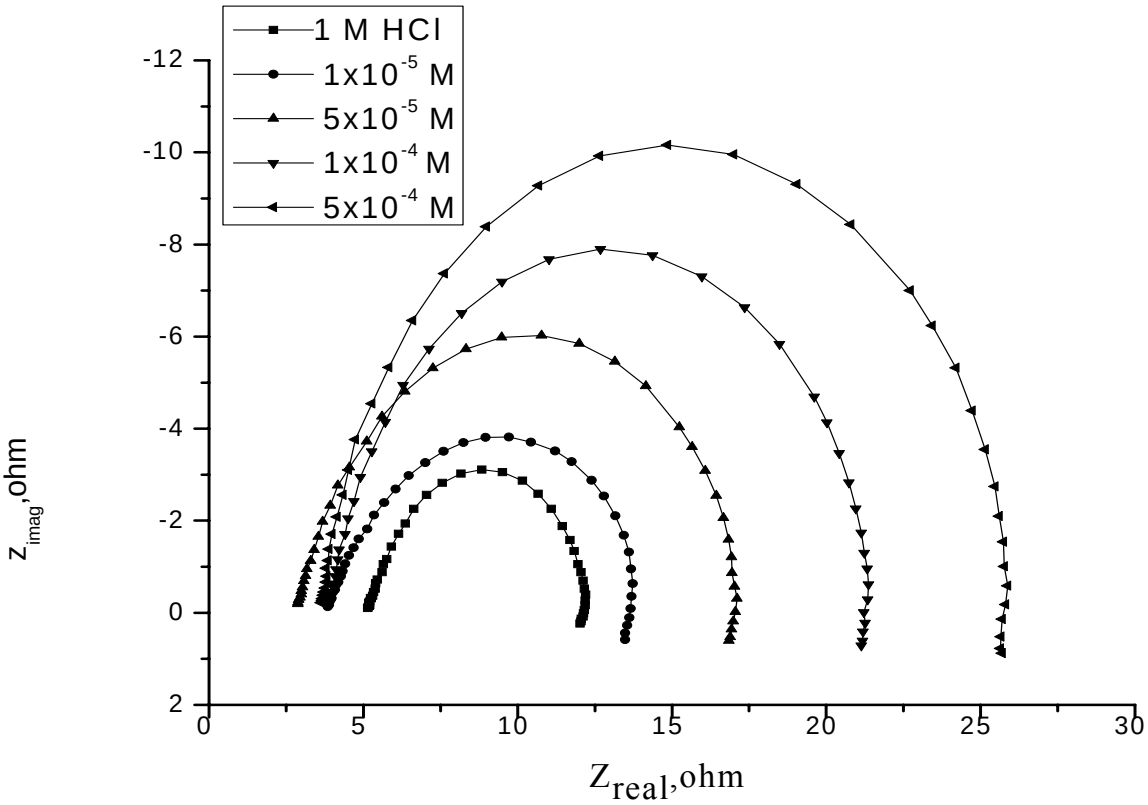

Fig (3.33): The Nyquist plots for aluminum-silicon in1 M HCl solution in the absence and presence of compound (I) at 25^{o}C.

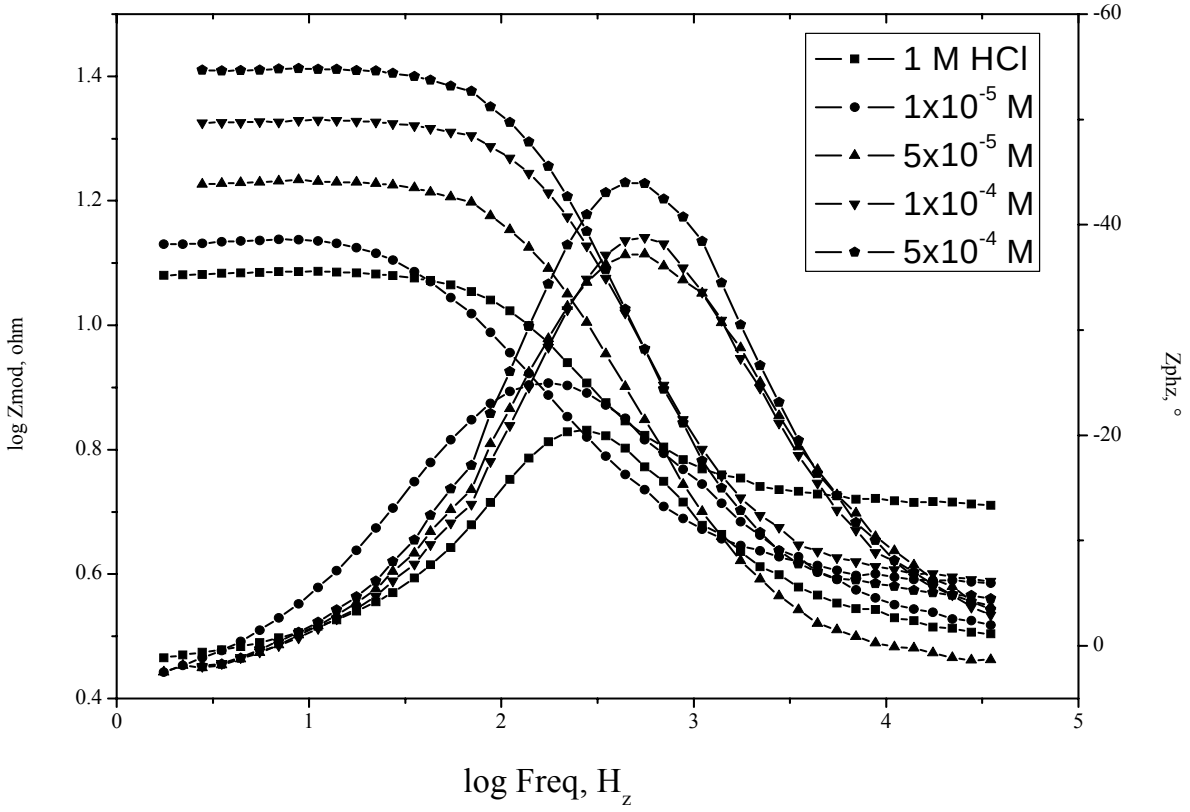

Fig(3.34): The Bode plots for aluminum-silicon in1 M HCl solution in the absence and presence of compound (I) at 25^{O}C

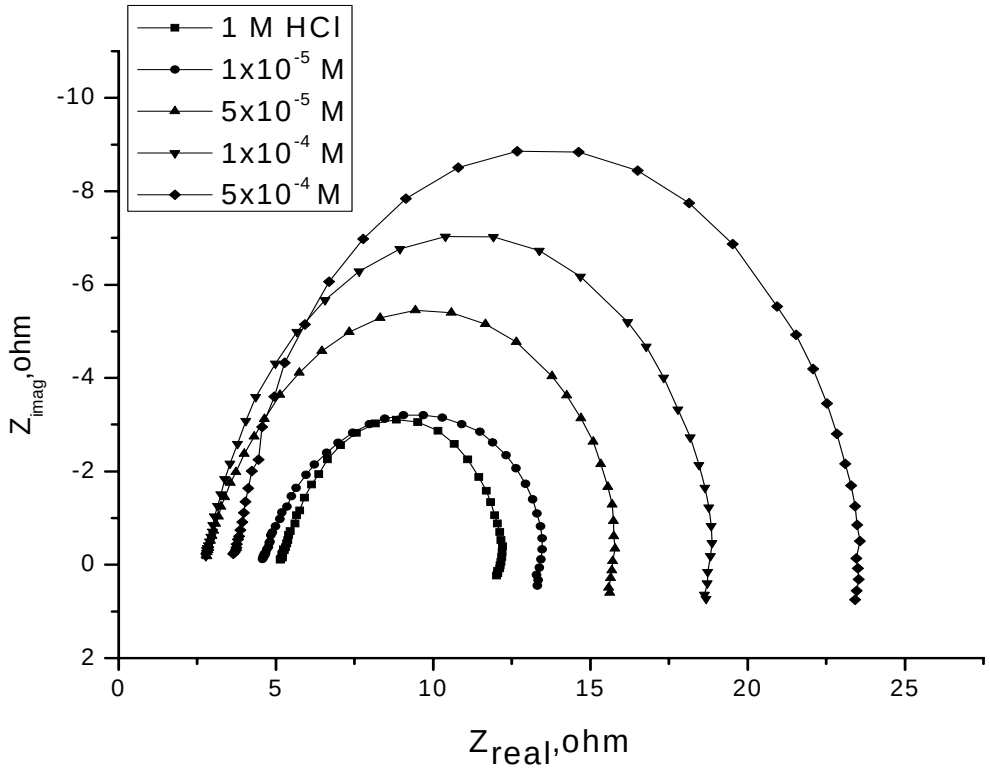

Fig (3.35): The Nyquist plots for aluminum-silicon in1 M HCl solution in the absence and presence of compound (II) at 25^{o}C.

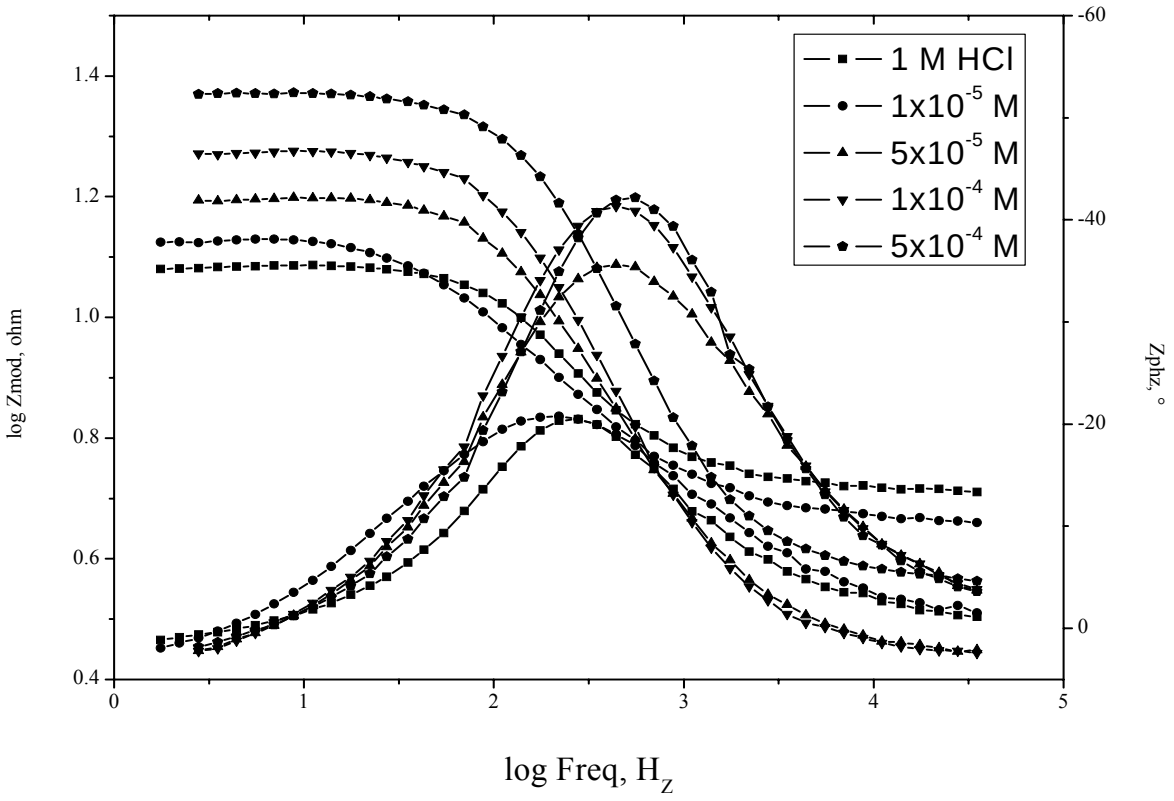

Fig(3:36): The Bode plots for aluminum-silicon in HCl solution in the absence and presence of compound (II) at 25^{O}C.

Table (3.14): Electrochemical kinetic parameter obtained by EIS technique of the corrosion of aluminum in 1 M HCL at different concentrations of investigated compounds at 25°C.

Inhibitor	Conc., M	C_{dl}, μF cm^{-2}	R_{ct}, ohm cm^2	θ	IE%
compound (I)	Blank	66.22	30.52	----	----
	$1x10^{-5}$	59.15	71.43	0.573	57.3
	$5x10^{-5}$	53.07	81.6	0.626	62.6
	$1x10^{-4}$	55.44	92.98	0.672	67.2
	$5x10^{-4}$	49.08	127.7	0.761	76.1
compound (II)	$1x10^{-5}$	61.57	75.03	0.593	59.3
	$5x10^{-5}$	54.55	76.06	0.599	59.9
	$1x10^{-4}$	53.35	89.95	0.661	66.1
	$5x10^{-4}$	52.79	127.6	0.761	76.1

Table (3.15): Electrochemical kinetic parameters obtained by EIS technique of the corrosion of aluminum-silicon in 1 M HCl at different concentrations of investigated compounds at 25 ^{o}C.

Inhibitor	Conc., M	$C_{dl,}$ µF cm^{-2}	R_{ct}, ohm cm^{2}	θ	IE%
compound (I)	Blank	66.22	30.52	----	----
	$1x10^{-5}$	59.4	8.935	0.253	25.3
	$5x10^{-5}$	59.04	13.31	0.499	49.9
	$1x10^{-4}$	45.38	16.78	0.602	60.2
	$5x10^{-4}$	44.37	21.44	0.689	68.9
compound (II)	$1x10^{-5}$	84.3	7.921	0.158	15.8
	$5x10^{-5}$	71.20	12.13	0.450	45.0
	$1x10^{-4}$	64.90	15.27	0.563	56.3
	$5x10^{-4}$	45.37	19.03	0.649	64.9

SECTION (C)

STUDYING THE CORRELATION BETWEEN INHIBITION ACTION AND CHEMICAL STRUCTURE OF THE INHIBITORS

Inhibition of corrosion of aluminum and aluminum-silicon alloy in 1 M HCl by the investigated compounds as measured by chemical and electrochemical techniques was found to depend on both the concentration and the nature of the inhibitor. The observed corrosion data in presence of the inhibitors namely:

1- The decrease of corrosion rate with increasing the concentration of the inhibitor.
2- The linear variation of weight loss with time.
3- The decrease in corrosion inhibition with increasing temperature.
4- The shift in Tafel lines to higher negative and positive potential values.

These observations indicate that the corrosion inhibition is due to adsorption of the inhibitors at the electrode-solution interface [144]. However, inhibition efficiency of the additive compounds depends on many factors [145], which include the number of adsorption active centers in the molecule and their charge density, molecular size, and mode of interaction with metal surface. It is generally believed that the adsorption of the inhibitor at the metal/ solution interface is the first step in the mechanism of inhibitor action in aggressive acid media.

3.7-Chemical structure of the inhibitors and its effect on the corrosion inhibition.

The inhibition efficiency depends on the type and number of active sites at the metal surface, the charge density, the molecular size of inhibitor, the metal-inhibitor interaction and the metallic complex formation [146]. Skeletal representation of the mode of adsorption of the investigated compounds on Al

and Al-Si alloy surfaces is shown in Fig. (3.37). As shown from this Figure, there are some donating atoms such as N and O atoms which can be serve as active centers. Compound (I) contains two active centers in addition to one more active centre (N atom of NH_2) and this compound lies flat on the Al and Al-Si alloy surfaces, so, more surface area was covered and hence, more inhibition efficiency was observed. Compound (II) has no substituent (H-atom),so , it has two active center only, In addition to the above the compound (I) has higher molecular size (203) than compound(II) (188), so more surface area was covered and hence, more inhibition efficiency was obtained.

The order of inhibition efficiency of the additives revealed by the weight loss method is further supported by potentiodynamic polarization measurement and AC impedance spectroscopy. The observed agreement among these independent techniques proves the validity of the results obtained and supports the explanation given for the effect of chemical structure on the inhibition action of the investigated compounds.

aminophenazone

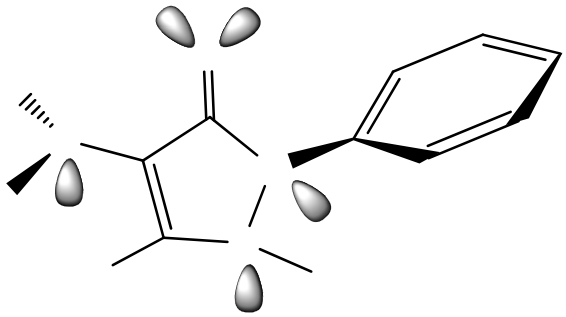

phenazone

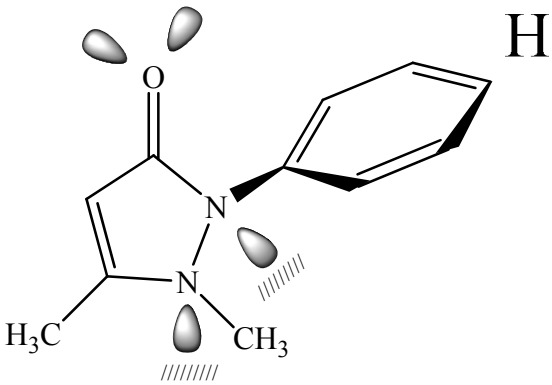

Fig.(3.37): Skeletal representation of the mode of adsorption of the investigated compounds.